UCLouvain

LOUVAIN
School of Management

Louvain School of Management

Energy Performance Characterization and Decarbonization Scenarios for University Buildings

Case of UCLouvain’s Stevin and Mercator Buildings

Authors : Apolline Chalmagne, Ugo Maquet
Supervisor : Bert Willems
Academic year 2025-2026
Final Thesis (TFE) for the purpose of obtaining the title of Master's Degree (60 ECTS) in Management Sciences
Daytime schedule

Abstract

The building sector accounts for approximately 40% of energy consumption and 36% of greenhouse gas emissions in the European Union, making it a central target of climate policy. In this context, UCLouvain has committed to achieving zero-carbon buildings by 2035, yet many of its campus buildings remain far below current energy performance standards. This master thesis focuses on two such buildings, Stevin and Mercator, and addresses the following research question: how can their actual energy performance be characterized, and which intervention scenarios would enable UCLouvain to meet its decarbonization targets?

The work is structured in two parts. The first characterizes the thermal behaviour of both buildings through climate-normalized consumption analysis, energy signatures, and residual analysis, using nine years of real monthly data (2017–2025). The second models three intervention scenarios, Slowheat, immediate Biomass and progressive Biomass, and evaluates their energy, environmental, and financial performance over a 10-year horizon using Net Present Value analysis, Monte Carlo simulation, and ETS-2 carbon pricing impact assessment.

Results show that the 2023 cavity wall insulation works reduced specific heating consumption by approximately 24% in both buildings, though this remains insufficient to meet the 2035 target. Among the intervention scenarios, immediate Biomass delivers the highest performance (2,951 MWh saved, 596 tCO_2 avoided, NPV of 122,887 € over 10 years), while Slowheat constitutes a valuable zero-CAPEX short-term measure. The analysis concludes that a combination of immediate Slowheat deployment and biomass connection from 2028 represents the most robust decarbonization pathway for UCLouvain.

Acknowledgements

First and foremost, we would like to thank our advisor, Professor Bert Willems, who helped us in the preparation and completion of this master thesis.

We would also like to thank Alexandre Duporte for kindly providing us with all the building data, without which this thesis would not have been possible.

Finally, a big thank you goes to our parents, without whom this emotionally rich year would not have been possible. We would also like to extend our warmest thanks to our friends, with whom we had the chance to share a truly exceptional and unforgettable year.

Thank you all for your contributions and support.

Note on AI usage

Claude (Anthropic), an AI language model, was employed for improved phrasing, language corrections for structural suggestions throughout the drafting process. All the work, from thinking to writing, remain the sole responsibility of the authors.

Contents

1 Introduction **1**

1.1 Overview . . . 1

1.2 Structure of the Thesis . . . 2

2 Literature Review **4**

2.1 Methods for Analyzing Real Energy Consumption in Buildings . . . 4

2.2 Degree-Days, Energy Signature and Overall Heat Loss Coefficient . . . 4

2.2.1 Theoretical Consumption Analysis: Degree-Day Approach . . . 5

2.2.2 Energy Signature and Overall Heat Loss Coefficient of Buildings . . . 6

2.3 Actual Performance, Theoretical Performance and Performance Gap . . . 6

2.4 Regulatory Energy Performance Indicators and Their Limitations . . . 7

2.5 Techno-Economic Analysis of Building Renovation . . . 8

2.6 The Slowheat Project . . . 9

2.7 Biomass Heating . . . 9

2.8 Net Present Value and Payback Period . . . 10

2.9 Monte Carlo Simulation . . . 10

2.10 EU Emissions Trading System for Buildings (ETS-2) . . . 11

3 Methodology **12**

3.1 Quantitative analysis of consumptions . . . 12

3.1.1 Scope, Data and Choice of Reference Area . . . 12

3.1.2 Synergrid Degree-Day Convention . . . 12

3.1.3 Climate Normalization and K Coefficient . . . 13

3.1.4 Energy Signature . . . 13

3.1.5 Residual Analysis: Two Complementary Readings . . . 15

3.1.6 Summary indicators . . . 15

3.1.7 PEB Comparison by Analogy . . . 16

3.2 Scenario Modelling and Financial Analysis . . . 17

3.2.1 Data collection and preparation . . . 17

3.2.2 Linear Regression and Trend Projection 18
3.2.3 Intervention Scenarios 18
3.2.4 Savings Calculation 19
3.2.5 Financial Analysis 20
3.2.6 Software and implementation 21

4 Results and Analysis 22
4.1 Remaining potential and economic analysis of further renovations 22
4.1.1 Trends in standardized consumption from 2017 to 2025 22
4.1.2 Energy performance of the buildings 23
4.1.3 Analysis of monthly residues 24
4.1.4 Cogeneration, primary energy factor and PEB classification 28
4.1.5 Prioritizing investments: what the economic analysis reveals 31
4.2 Energy and Financial Performance of Intervention Scenarios 32
4.2.1 Historical Consumption (2017–2025) 32
4.2.2 Predicted Consumption by Scenario 33
4.2.3 Energy Savings and CO_2 Reductions 33
4.2.4 Financial Analysis 35
4.3 Limitations 38
4.3.1 Limitations of the energy performance characterization 38
4.3.2 Limitations of the scenario modelling and financial analysis 39

5 Conclusion 40
5.1 Perspectives 41

A UCLouvain's internal data on the Stevin and Mercator buildings 47

B Annual Heating Consumption 48

C Heating Consumption Raw Data 50
Heating Consumption Data 50

Chapter 1

Introduction

1.1 Overview

In a world where the notions of sustainable development and ecological and energy transition are increasingly prominent, the question of energy consumption in tertiary buildings has been the subject of numerous studies. At the European level, buildings account for approximately 40% of energy consumption and are responsible for 36% of energy-related emissions [1]. The building sector therefore represents a major lever in terms of reducing energy consumption. The importance accorded to renovation in energy transition policies then becomes self-evident. In this context, the existing building stock is a priority, as it will remain in service for decades to come.

Tertiary buildings differ from residential buildings in having highly heterogeneous usage profiles that depend on the activity carried out within them [2, 3]. Energy consumption is notably influenced by occupancy schedules, the operating conditions of technical systems, ventilation, etc [4, 5, 6]. Consequently, the analysis of energy consumption in this type of building must use sufficiently complex models in order to integrate climatic conditions, actual building usage, and so-called free heat gains linked to operating conditions [7, 8].

The analysis of a university building is even more complex, given its more diverse functions, including laboratories, technical rooms, and varied class schedules, to name but a few. Furthermore, the energy renovation of existing buildings is not straightforward, as it must account for the physical, technical, and operational constraints specific to the existing building [5]. The choice of renovations must cover the building envelope and the adaptation of technical systems, while taking into account the economic feasibility of the renovation [5, 6]. Cost-optimal approaches allowing different renovation measures to be compared in terms of investment costs, energy savings, and lifecycle profitability will be discussed in Section 2.5 [1, 4]. As large public institutions managing extensive and often aging building stocks, universities are particularly exposed to these pressures, facing a dual challenge: reducing their energy footprint while preserving the quality and continuity of their academic activities.

The University of Louvain-la-Neuve (UCLouvain) is no exception. Its campus, built largely in the 1970s, hosts a dense network of buildings whose energy performance is far below current standards. Among these, two buildings stand out as the focus of this master thesis: Stevin (SC04) and Mercator (SC10). Both have recently been the subject of cavity wall insulation works carried out between 2022 and 2023, with a total treated surface of approximately 1,445 m^2 for Stevin and 1,273 m^2 for Mercator. All the data used, provided by UCLouvain, is available in the Appendix A. While these interventions represent a meaningful first step, they remain partial, several façade sections could not be treated due to insufficient cavity width or structural constraints, and the question of residual energy consumption remains open. What is more, these renovations are not sufficient to meet the 'Plan Transition' established by UCLouvain, which aims to achieve zero-carbon buildings by 2035 [9]. Further work is therefore needed to reduce the energy consumption of the Stevin and Mercator buildings.

Ultimately, this research aims to answer the following question:

How can the actual energy performance of the Stevin and Mercator buildings be characterized, and which intervention scenarios would enable UCLouvain to meet its decarbonization targets by 2035 ?

1.2 Structure of the Thesis

The first part of this master thesis focuses on the characterization of the actual energy performance of the Stevin and Mercator buildings. Starting from nine years of real monthly heating consumption data (2017–2025), a climate-normalized analysis is carried out using the Synergrid degree-day convention to compare inter-annual performance independently of meteorological variations. The overall heat loss coefficient K and its equivalent U_{global} are computed to quantify the intrinsic thermal behaviour of each building. The energy signature, based on a linear regression of monthly consumption against outdoor temperature, provides a complementary characterization of thermal losses and allows the effect of the renovation works carried out in 2023 to be assessed. A residual analysis further distinguishes structural changes in building performance from seasonal operational effects. Finally, an analogy-based comparison with regulatory energy performance indicators (Ew and Espec) is used to position the buildings on the Walloon certification scale. The diagnostic is then extended through a prospective economic analysis comparing six retrofit scenarios ranging from low-cost operational quick wins to deep envelope and system renovations, in order to assess the trade-off between short payback measures and more ambitious but less profitable interventions.

The second part of this master thesis, focuses on quantitative scenario modelling for the Stevin and Mercator buildings. Starting from nine years of real monthly heating consumption data (2017–2025), a linear regression is fitted to project the baseline consumption trend over a 10-year horizon (2026–2035). Three intervention scenarios are then modelled: Slowheat, which assumes a 50% reduction in heating consumption through setpoint management; immediate Biomass, which eliminates fossil heating from January 2028 onwards in line with UCLouvain's planned biomass plant; and progressive Biomass, which models a gradual three-year transition. For each scenario, cumulative energy savings, CO_2 reductions, and financial savings are computed. The financial analysis further includes a Net Present Value assessment, an ETS-2 carbon pricing impact analysis, and a Monte Carlo simulation to quantify uncertainty around gas price assumptions.

Chapter 2

Literature Review

2.1 Methods for Analyzing Real Energy Consumption in Buildings

The energy consumption of a building can be assessed with varying degrees of complexity. The simplest approach consists of measuring consumption directly from meters or energy bills, but does not account for climatic variations or complex usage patterns, making direct year-to-year comparisons potentially misleading.

Several normalization methods exist. A first class of methods proposes a whole-building approach integrating explanatory variables such as weather or occupancy [10], while others follow the same logic of adjusting reference consumption baselines [7]. Energy signatures statistically relate consumption to a climatic variable such as outdoor temperature, with both their interest for prediction and their limitations for physical interpretation being well documented in the literature [11]. They have also been used to estimate effective U-values and heat loss coefficients [12, 13]. More complex dynamic models allow for a finer representation of thermal inertia and solar gains, but require more data and expertise [10].

Among all the methods presented, the degree-day approach emerges as a relevant compromise for the analysis of existing buildings. It is simple, requires little data, is compatible with monthly consumption figures, and allows correction for the main climatic effect on heating needs. Its uncertainties decrease when the analysis covers longer periods, such as a full heating season [8, 14].

2.2 Degree-Days, Energy Signature and Overall Heat Loss Coefficient

This section presents in more detail three methods used to analyze the energy performance of a building.

2.2.1 Theoretical Consumption Analysis: Degree-Day Approach

The degree-day approach assumes that heating needs are proportional to the difference between a reference indoor temperature and the outdoor temperature, and only arise when the outdoor temperature falls below a threshold value.
The degree-day score (DD) is calculated over a given period as:

$$DD = \sum (T_{ref} - T_{ext,avg}) \tag{2.1}$$

where T_{ref} is the reference indoor temperature and $T_{ext,avg}$ the daily average outdoor temperature. Only days where $T_{ref} > T_{ext,avg}$ are taken into account.

Climate Normalization of Energy Consumption

The degree-day approach is primarily used to correct energy consumption figures in order to compare them across years with different meteorological conditions:

$$Q_{corr} = Q_{mes} \cdot \frac{DD_{normal}}{DD_{year}} \tag{2.2}$$

where Q_{mes} is the measured consumption, DD_{year} the degree-days of the year under study, and DD_{normal} those of a reference climatic year. This correction is essential for evaluating the actual effect of a renovation. However, heating needs do not depend solely on the indoor-outdoor temperature difference: solar gains and dynamic effects also directly influence heating needs and the estimation of heat losses, which purely stationary models do not always capture correctly [15].

Reference Temperature and Equivalent Temperature

The reference temperature is a key variable in the degree-day approach, as it is the basis on which the method's score is calculated. In classical degree-day methods, the reference temperature is typically set between 18 °C and 20 °C. However, several recent studies show that this assumption may be insufficient to correctly represent actual heat exchanges.

The work of Senave et al. shows that heat exchanges depend not only on outdoor air temperature but also on solar radiation, long-wave infrared radiation towards the sky, surface temperatures, and the thermal inertia of walls, among other factors. The study demonstrates that the direct use of air temperatures leads to significant errors in the estimation of the overall heat transfer coefficient, with discrepancies reaching approximately 19%, and up to 41% in some uninsulated cases [16].

2.2.2 Energy Signature and Overall Heat Loss Coefficient of Buildings

As discussed in Section 2.1, the energy signature of a building is the relationship between heating consumption and the outdoor climatic conditions. It constitutes an analysis tool for characterizing the overall thermal behaviour of the building. In standard models, it is expressed as follows:

$$Q_{cons} = f(T_{ref}, T_{ext}) \tag{2.3}$$

or alternatively using the degree-day method:

$$Q_{cons} = f(DD) \tag{2.4}$$

This consumption is also often approximated by a simple linear law:

$$Q_{cons} = H \cdot (T_{ref} - T_{ext}) + b \tag{2.5}$$

where Q_{cons} $[W]$ is the amount of heat consumed (if the energy consumption over a period is related, it is referred to $[Wh]$) , H is the overall heat loss coefficient $[W/K]$, and b the consumption independent of climatic conditions (domestic hot water, base loads, etc.). The slope H gives the sensitivity of the building to outdoor conditions: the greater the thermal losses, the steeper the slope. The energy signature is thus a tool for estimating thermal losses, comparing buildings, identifying consumption drifts, and evaluating the effect of a renovation.

Overall Heat Loss Coefficient

The overall heat loss coefficient (HLC) represents the heat lost by the building per degree Kelvin of indoor-outdoor temperature difference. It is expressed as:

$$HLC = \sum U_i A_i - H_{conv} \tag{2.6}$$

where U_i is the thermal transmittance of wall i, A_i its surface area, and H_{conv} the convective heat transfer losses. While the HLC is classically determined from envelope characteristics, it can also be estimated from measured data under real operating conditions, accounting for heating consumption, indoor and outdoor temperatures, and meteorological time series [17]. Dynamic models such as ARX and RC models further improve this estimation by accounting for thermal inertia, transient effects, and solar gains [16, 15].

2.3 Actual Performance, Theoretical Performance and Performance Gap

The energy performance derived from design-phase calculations relies on standardized assumptions (occupancy conditions, setpoints, schedules, etc.), which allows comparison across buildings

but does not necessarily predict actual operation faithfully [18]. Theoretical performance is useful for verifying compliance with minimum requirements, but its results should not be directly compared with actual operating conditions. Actual performance, by contrast, depends on schedule variability, occupancy density, user behaviour, control settings, and maintenance strategies. The gap between prediction and measurement captures precisely the complexity of these sub-systems and interactions, and measured consumption can reach up to 2.5 times the predicted value [3].
This discrepancy is referred to as the *performance gap*. What is more, this gap is not merely “noise” around the calculations, often significant difference exists between predicted and measured performance once the building is in operation [18]. A useful classification distinguishes: (i) the *regulatory gap* (between regulatory calculation and measurement), (ii) the *static gap* (between a performance model and measurement), and (iii) the *dynamic gap* (after calibration and longitudinal analysis). The type of gap at stake depends on the theoretical reference retained [18].
For tertiary buildings, the *performance gap* can be particularly pronounced. The complexity of uses (multiple occupants, IT equipment, specific rooms, intermittent occupancy, extended schedules) quickly renders standard assumptions far from reality. Based on post-occupancy data, discrepancies can arise from unrealistic assumptions about occupancy and facility management, and current tools still struggle to correctly represent the impact of occupants and building management [2].
The relevance of this topic goes beyond simple diagnosis: the quantification of savings and the robustness of renovation policies are directly linked to it. Energy certificates rely on comparative standards and assumptions, making them more of a "design certification" than a measure of actual operation. This highlights not only the gap between theoretical and actual consumption, but also the gap between theoretical savings and those actually achieved after renovation [19].
The analysis of actual consumption is therefore not in competition with the regulatory approach but complementary to it, helping to understand the causes of the gap, consolidate assumptions, and better prioritize actions.

2.4 Regulatory Energy Performance Indicators and Their Limitations

Energy performance (EP) indicators primarily serve a standardization objective: they provide a common regulatory language for describing and comparing the energy performance of different buildings, partly independently of usage variations. In line with the European energy certification framework, certificates aim to inform, compare, and support policies such as minimum standards and renovation trajectories [20].

EP Indicators: A Common Basis for Setting Requirements and Comparing Performance

Within this framework, Walloon regulation uses two key indicators [20]. First, **Ew**, which is the ratio between the annual primary energy consumption[1] of the building (or PEB unit) and a reference consumption, multiplied by 100. The lower the Ew, the more energy-efficient the building. Second, **Espec**, which is the specific primary energy consumption per heated floor area, and constitutes the basis for the energy label assigned on the certificate [20]. These indicators translate performance through a shared methodology covering envelope, systems and efficiencies, and are used to set requirements, verify compliance, and structure public policies.

However, standardized comparison is both a strength and a limitation. These indicators rely on calculation conventions, standard usage profiles and operating conditions, which connects to the *performance gap* discussed in Section 2.3. The EPBD directive requires certification, but leaves the precise calculation methodology to Member States, reinforcing the idea that EP certificates are primarily a regulatory object rather than a direct reflection of reality [21].

This is precisely what leads to the *performance gap* discussed in Section 2.3. Based on a large sample of around 200,000 dwellings, actual consumption in low-performing buildings is often lower than the theoretical prediction, while in high-performing buildings it can exceed it [21, 22]. In general, theory tends to overestimate the consumption of average or poorly efficient buildings, and may underestimate that of new or renovated ones.

2.5 Techno-Economic Analysis of Building Renovation

A single indicator is not sufficient to correctly evaluate energy renovations. Renovations involve trade-offs between energy performance, climate impact, costs, feasibility, and quality of use. A multi-criteria approach structured around primary energy consumption, greenhouse gas emissions, and annualized lifecycle costs is therefore recommended [6]. This allows renovation scenarios of increasing ambition to be compared consistently, avoiding over-optimization of a single dimension at the expense of others.

From an economic standpoint, a lifecycle cost analysis covering investment, energy costs with taxes, and operation and maintenance is recommended, subsequently converted into annualized costs. The assumptions used (discount rate, study horizon, component lifespan, and energy price trajectory) strongly influence the profitability of renovations, hence the importance of scenario and sensitivity analyses. It is also essential to distinguish the reference case from an *anyway renovation* so as not to attribute costs that would have existed regardless [6].

Within this economic framework, a distinction is made between quick wins and deep renovations. Quick wins regroup no-cost or low-cost measures such as control adjustments, schedule optimization, or setpoint changes, generating rapid savings with minimal disruption. Savings from

[1]The annual primary energy consumption means the yearly energy demand of the building after converting all delivered energies (heating, domestic hot water, ventilation, auxiliaries, lighting, etc) into primary energy, using regulatory conversion factors.

such measures may remain limited, whereas measures requiring significant capital can achieve much higher gains [5].
Deep envelope renovations allow for larger reductions in heating needs, but their profitability depends heavily on energy price trajectories and the discount rate. Research conducted at UCLouvain shows that announced payback periods can vary significantly depending on the chosen reference and energy cost evolution scenarios [23].

2.6 The Slowheat Project

The SlowHeat project is a transdisciplinary research initiative funded by the *Cocréation programme* of Innoviris, conducted jointly by UCLouvain (LOCI+LAB), ULB (IGEAT) and the association Habitat et Participation [24]. Its central objective is to explore a new heating practice, summarized by the question: can we heat bodies rather than buildings?
The main outcome of the project is slowheating, a heating practice built around a fundamental distinction between two objectives: maintaining the thermal well-being of occupants, and ensuring the minimum ambient conditions necessary for the building's healthiness [25]. It is structured around four axes: openness to diverse heating solutions, multimodality in the means used, conscious control of energy consumption, and sobriety by systematically favouring the least energy-intensive options [25].
The experimental results of the project showed a 57% average reduction in heating energy consumption after three winters of experimentation, reaching a mean indoor temperature close to 15°C [25]. In this master thesis, a conservative factor is therefore applied relative to the 57% reported, and the approach is analyzed from a cost-benefit perspective for the Stevin and Mercator buildings.

2.7 Biomass Heating

Biomass designates all organic matter that can be converted into energy. It exists in three main forms : Solid (e.g. straw, wood chips, logs), liquid (e.g. vegetable oils, bioalcohols) and gaseous (e.g. biogas). Biomass originates from forestry, agricultural or fermentable sources [26]. Among the various conversion pathways, the most relevant for building heating applications is combustion, which produces heat through the complete oxidation of the fuel. The resulting hot water can be distributed directly through a district heating network, making it a straightforward replacement for conventional gas-fired boilers [26].
Biomass is considered carbon neutral, since during combustion it emits the CO_2 that was previously absorbed from the atmosphere during its growth, thereby contributing to climate change mitigation rather than adding new carbon to the cycle (Nunes et al., 2019). This distinguishes it fundamentally from fossil fuels such as natural gas, which release carbon that has

been locked underground for millions of years. In the case of recycled wood waste specifically, this argument is further strengthened: the material has already fulfilled a first use cycle, and its energetic valorization avoids the emissions that would result from its disposal or degradation [27].
In the context of this master thesis, the biomass scenario is modelled based on the UCLouvain biomass project planned for 2027. The plant will be fuelled by 55,000 tonnes per year of Class B wood waste, comprising elements such as beams, doors and deconstruction materials, primarily collected from Walloon recyparcs in a short local supply chain [28]. UCLouvain opted for biomass on grounds of reliability and cost stability, with the plant expected to cover nearly 100% of the campus's annual energy needs (40 GWh of heat and 26 GWh of electricity) from winter 2027 onwards [28][29].

2.8 Net Present Value and Payback Period

When evaluating energy efficiency investments, the simple payback period is often an insufficient metric on its own, as it does not account for the time value of money nor for cash flows occurring beyond the recovery threshold [30]. The Net Present Value (NPV) is therefore the primary decision criterion used in this thesis. It is defined as the present value of all cash flows associated with a project, both positive and negative.
A positive NPV indicates that the present value of the generated cash flows exceeds the initial investment, meaning the project creates value and should be undertaken. In this master thesis, the cash flows correspond to annual energy savings, computed over a 10-year horizon [30].
The choice of discount rate is among the most sensitive parameters in building energy efficiency evaluations, with an outsized impact on long-duration projects, a particularly relevant consideration given the lifespan of building infrastructure [31]. The payback period is additionally reported as a complementary indicator, useful for assessing short-term financial feasibility.

2.9 Monte Carlo Simulation

When a key input parameter is uncertain, a single deterministic scenario may give a misleading picture of a project's financial viability. Monte Carlo simulation addresses this by using random sampling and statistical modelling to estimate the range of possible outcomes of a complex system [32]. The method consists of three main steps: modelling the uncertain variable as a probability distribution, repeatedly sampling from that distribution, and tallying the resulting outputs to produce a statistical summary of outcomes [32]. The uncertain variable is typically characterized by a mean μ and a standard deviation σ, which define the shape and spread of the distribution from which random draws are made [32]. By running a large number of simulations, this approach yields not a single estimate but a full distribution of possible outcomes, allowing decision-makers to assess the probability and magnitude of different scenarios [33].

2.10 EU Emissions Trading System for Buildings (ETS-2)

The EU Emissions Trading System (ETS) is a carbon pricing mechanism that operates on a cap-and-trade principle, requiring emitters to surrender allowances for each tonne of CO_2 they emit. As part of the 2023 revision of the ETS Directive, a new and separate system, referred to as ETS-2, was created to extend carbon pricing to sectors not previously covered, namely buildings, road transport and small industry [34]. Unlike the original ETS, where large industrial emitters are regulated directly, the ETS-2 will operate upstream: it is fuel suppliers who will be required to monitor, report and surrender allowances for the emissions embedded in the fuels they distribute. The system is set to become fully operational in 2028, with the cap designed to bring emissions in the covered sectors down by 42% by 2030 compared to 2005 levels [34]. For institutions such as UCLouvain that consume natural gas for heating, this mechanism will translate into an additional carbon surcharge on their energy bills from 2028 onwards, further strengthening the financial case for switching to low-carbon heating alternatives.

Chapter 3

Methodology

3.1 Quantitative analysis of consumptions

3.1.1 Scope, Data and Choice of Reference Area

The analysis focuses on two university buildings at UCLouvain in Louvain-la-Neuve, Stevin and Mercator, both connected to the same centralized district heating network. The Stevin building, constructed in 1971, has a Net Room Area (NRA) of 8,249 m^2, while Mercator has a NRA of 6,035 m^2.

The data used include heating and electricity consumption over the period 2017–2025, monthly temperatures from the Uccle weather station, architectural floor plans (PAT), and boiler room technical data. The DIU documents also allow identification of the post-insulation works carried out in March 2023 on the facades of Stevin and Mercator, as well as the renovation of wing A of Stevin.

Among the various available surface area conventions, the NRA is retained as an approximation of the Ach, as it excludes walls and unheated technical rooms while faithfully representing occupied spaces. The Ach/NRA discrepancy is estimated at 5–10%, a source of uncertainty that is acknowledged and discussed in Section 4.1.4.

3.1.2 Synergrid Degree-Day Convention

The Synergrid convention defines the climate normalization standard used by the Belgian natural gas sector [35]. According to this convention, the degree-day for a given day J is:

$$DD(J) = \max(0,\ 16.5 - T_{avg}(J)),$$

where the threshold of 16.5°C results from a conventional indoor setpoint temperature of 20°C reduced by approximately 3.5°C to account for typical internal and external free heat gains. To integrate the thermal inertia of the building, Synergrid uses weighted equivalent degree-days:

$$DD_{eq}(J) = 0.6 \cdot DD(J) + 0.3 \cdot DD(J-1) + 0.1 \cdot DD(J-2) \tag{3.1}$$

The thermal memory of the structure over three rolling days is thus modelled by the coefficients 0.6 / 0.3 / 0.1, established empirically on the Belgian building stock. The annual total for a climatically normal year, based on the rolling thirty-year reference period, is $DD_{normal} = 2187$. For the period 2017–2025, the degree-days are calculated from monthly average temperatures (see Appendix C) provided by UCLouvain's technical services, and amount to 2064, 1896, 1963, 1674, 2113, 1742, 1830, 1942 and 1973 respectively, corresponding to deviations from the normal ranging from −23.5% (mild winter of 2020) to −3.4% (2021).

3.1.3 Climate Normalization and K Coefficient

In order to compare inter-annual performance independently of meteorological variations, each annual consumption must be normalized as follows:

$$Q_{\text{norm}} = Q_{\text{annual}} \cdot \frac{DD_{\text{normal}}}{DD_{\text{year}}} \tag{3.2}$$

All years are thus brought to an equivalent climatic severity. The normalized specific consumption is expressed in kWh/m^2.
The empirical heat loss coefficient is defined as:

$$K = \frac{Q_{\text{annual}}\ [\text{kWh}]}{DD_{\text{year}} \cdot NRA\ [\text{m}^2]} \quad \left[\frac{\text{kWh}}{\text{DD} \cdot \text{m}^2}\right] \tag{3.3}$$

This coefficient depends on the annual consumption measured at the building's entry meter. It therefore globally integrates envelope losses, ventilation losses, internal distribution network losses, and regulation losses, reduced by internal and external free heat gains.
It can subsequently be converted into an equivalent global thermal transmission coefficient:

$$U_{\text{global}} = K \cdot \frac{1000}{24} \quad \left[\frac{\text{W}}{\text{m}^2 \cdot \text{K}}\right] \tag{3.4}$$

This conversion derives from the following dimensional equivalence: one degree-day corresponds to a temperature difference of ~1°C maintained over 24 hours.

3.1.4 Energy Signature

The energy signature plots monthly specific consumption as a function of monthly average outdoor temperature:

$$Q_{\text{month}} = a \cdot T_{\text{ext}} + b \tag{3.5}$$

This linear regression is based on the assumption of a quasi-stationary regime and allows several physical parameters to be extracted. The slope a (kWh/m^2/°C/month) is proportional to the overall heat loss coefficient:

$$H = H_T + H_V \tag{3.6}$$

where H_T [W/K] represents transmission losses through the building envelope (opaque walls, glazing and thermal bridges), and H_V [W/K] represents losses due to ventilation and air infiltration. The conversion to W/m^2·K is performed as follows:

$$H = |a| \cdot \frac{1000}{24 \cdot 30.44} \quad \left[\frac{\mathrm{W}}{\mathrm{m}^2 \cdot \mathrm{K}}\right] \tag{3.7}$$

This coefficient H, normalized by the net room area (NRA), corresponds to the U_{global} coefficient defined in Section 3.1.3. The energy signature and the K coefficient therefore constitute two distinct estimators of the same physical quantity, which will allow cross-validation if convergence is observed.

The intercept b (kWh/m^2) represents the consumption extrapolated to zero outdoor temperature. It integrates in particular the permanent losses of the internal distribution network and auxiliaries, reduced by average free heat gains.

The non-heating temperature is given by:

$$T_{\mathrm{nc}} = -\frac{b}{a} \tag{3.8}$$

It corresponds to the outdoor temperature above which the building theoretically no longer consumes heating. It can also be interpreted as a composite indicator:

$$T_{\mathrm{nc}} = T_{\mathrm{setpoint}} - \frac{\text{Free heat gains}}{H} \tag{3.9}$$

The coefficient of determination R^2 of the signature measures the fraction of variance in consumption Q explained by T_{ext}. It is therefore interpreted as an indicator of thermal predictability. A high R^2 reflects consumption that is well explained by weather conditions and consistent regulation. Conversely, a low R^2 indicates the influence of other factors, such as restart sequences, malfunctions, variable occupancy, or envelope heterogeneity.

However, R^2 is not an indicator of energy performance: it measures the quality of the statistical fit, not the quality of the envelope. A passive insulation renovation may reduce $|a|$ and $|b|$ without necessarily modifying R^2, since the correlation is invariant under affine transformations. The effect of renovation works must therefore be assessed primarily from the slope a, and secondarily from the intercept b, rather than from R^2.

3.1.5 Residual Analysis: Two Complementary Readings

The differences between measured consumption and consumption predicted by the energy signature, referred to as residuals, provide two physically distinct types of information depending on the chosen reference signature.

Residuals Relative to a Fixed Reference Signature

A single reference signature is computed over the pre-renovation period 2017–2022:

$$\hat{Q}_{\text{ref}}(T) = a_{\text{ref}} \cdot T + b_{\text{ref}} \tag{3.10}$$

This regression is established from all monthly (T, Q) pairs available over the reference period. For each post-renovation month, the relative residual is defined as:

$$\varepsilon_i^{\text{ref}} = \frac{Q_i - \hat{Q}_{\text{ref}}(T_i)}{\hat{Q}_{\text{ref}}(T_i)} \times 100 \quad [\%] \tag{3.11}$$

Q_i being the monthly specific heating consumption of the building, this deviation compares actual consumption with what would have been predicted for the building in its initial state at the same outdoor temperature. A systematically negative residual after renovation therefore indicates an energy saving attributable to a structural change, and constitutes an estimator of the energy gain associated with the renovation works.

Residuals Relative to Each Year's Own Signature

An independent regression is also computed for each year:

$$\hat{Q}_y(T) = a_y \cdot T + b_y \tag{3.12}$$

The monthly residual then becomes:

$$\varepsilon_{i,y}^{\text{own}} = \frac{Q_{i,y} - \hat{Q}_y(T_{i,y})}{\hat{Q}_y(T_{i,y})} \times 100 \tag{3.13}$$

This no longer measures the structural effect, since it is absorbed by the annual parameters a_y and b_y, but rather seasonal operational biases: January restart effects, mid-season behaviour, or reproducible patterns independent of the envelope.

3.1.6 Summary indicators

The mean absolute error is defined as:

$$\text{MAE} = \frac{1}{n} \sum_{i=1}^{n} |\varepsilon_i|$$

and the root mean square error as:

$$\text{RMSE} = \sqrt{\frac{1}{n}\sum_{i=1}^{n}\varepsilon_i^2}$$

These two indicators characterize the dispersion of the residuals. The RMSE expressed in absolute terms, for example in kWh/m^2, reflects thermal noise in physical units, while the relative RMSE, expressed as a percentage, allows comparison across buildings or periods with different consumption levels. The joint interpretation of the absolute RMSE and R^2 thus avoids the erroneous conclusion that a stable R^2 implies an absence of renovation effect.

3.1.7 PEB Comparison by Analogy

The E_{spec} (kWh$_{ep}$/m^2/year) and E_w, defined in Section 2.4, require the conversion of final consumption into primary energy using the regulatory primary energy factors f_p.
For electricity, the factor is set by the Walloon PEB Guide [36] to:

$$f_{p,\text{elec}} = 2.5 \tag{3.14}$$

For heat supplied by the UCLouvain network, the calculation is less straightforward. The network combines two sources of different natures: gas-fired smoke-tube boilers with an efficiency of:

$$\eta_{\text{boiler}} = 0.90 \tag{3.15}$$

giving:

$$f_{p,\text{boiler}} = \frac{1}{0.90} = 1.111 \tag{3.16}$$

and two gas cogeneration units of respective capacities 3.42 MW and 5.79 MW, installed in 2010. Cogeneration simultaneously produces heat and electricity from gas, which requires choosing an allocation method for the gas consumed between these two useful outputs.
The actual efficiencies of the engines are extracted from monthly meter readings from internal files, over the period January–June 2025:

$$\eta_{\text{th}} = 40.0\% \qquad \eta_e = 31.9\% \qquad \eta_{\text{total}} = 71.9\%$$

These values, lower than the nominal efficiencies of 2010 estimated at 87.7%, may reflect the aging of the installation after 15 years of service. Three allocation methods are compared.

Default Method

Cogeneration is assimilated to pure gas heat production:

$$f_{p,\text{cogen}} = 1.0 \tag{3.17}$$

This assumption ignores the cogeneration effect and therefore constitutes a conservative approach.

Proportional PER Method

The gas consumed is allocated in proportion to the useful thermal and electrical outputs:

$$f_{p,\text{cogen}}^{\text{PER}} = \frac{1}{\eta_{\text{th}} + \eta_e} \tag{3.18}$$

Substitution Method

Cogeneration is credited with the electricity avoided from the grid:

$$f_{p,\text{cogen}}^{\text{SUB}} = \frac{1}{\eta_{\text{th}}} - \left(\frac{\eta_e}{\eta_{\text{th}}}\right) \cdot f_{p,\text{elec}} \tag{3.19}$$

The average primary energy factor of the network is then calculated as a weighted average by the cogeneration share, estimated at ~30% in 2025:

$$f_{p,\text{network}} = p_{\text{cogen}} \cdot f_{p,\text{cogen}} + (1 - p_{\text{cogen}}) \cdot f_{p,\text{boiler}} \tag{3.20}$$

The calculation of E_{spec} uses the surface A_{ch}, i.e. the heated area of the protected volume according to the Belgian PEB convention. This is estimated from the PAT floor plans at 6,427 m^2 for Stevin and 5,458 m^2 for Mercator.
This analogy-based approach does not replace an official PEB calculation with a detailed envelope audit, but it allows the buildings to be positioned on the regulatory scale, with an uncertainty that is acknowledged and discussed in Section 4.1.4.

3.2 Scenario Modelling and Financial Analysis

This section presents the quantitative methodology used to assess the energy and financial efficiency of three intervention scenarios for the Stevin and Mercator buildings: Slowheat, immediate biomass, and progressive biomass.

3.2.1 Data collection and preparation

The analysis is based on real monthly heating consumption data (in MWh) for both Stevin (SC04) and Mercator (SC10) , covering the period from January 2017 to December 2025, representing nine full years of observations and a total of 108 data points per building (see Appendix C). These data were provided directly by UCLouvain's technical services (ADPI/SEPI) and constitute the empirical foundation of the model. Negative values, which occasionally appear due to measurement artefacts in the building management system, were retained as recorded rather than zeroed out, in order to preserve the integrity of the regression fit. Each monthly observation was associated with a proper timestamp (first day of the month) to enable time-series operations.

3.2.2 Linear Regression and Trend Projection

Principle. To project future consumption under a business-as-usual reference scenario (denoted *Normal*), a linear regression is fitted to each monthly time series. The explanatory variable is the number of days elapsed since the first observed month; the response variable is the monthly consumption in MWh. The model reads:

$$\hat{C}(t) = \beta_0 + \beta_1 \cdot t \tag{3.21}$$

where t is the number of days since January 2017 and $\hat{C}(t)$ is the predicted monthly consumption in MWh. The coefficients β_0 (intercept) and β_1 (slope) are estimated by ordinary least squares using `scikit-learn`'s `LinearRegression` class. Model performance is assessed via the coefficient of determination R^2 and the root mean squared error (RMSE).

Building	R^2	RMSE (MWh/month)	Trend (MWh/year)	Direction
Stevin	0.025	49.47	−3.0	Slight decrease
Mercator	0.020	23.68	−1.3	Slight decrease

Table 3.1: Linear regression parameters per building (monthly data, 2017–2025)

Regression results. The low R^2 values (2–3 %) are expected for monthly heating data dominated by seasonal variability: the linear regression captures the *long-term trend*, not the seasonal pattern. The negative slopes (−3.0 and −1.3 MWh/year for Stevin and Mercator respectively) reflect a gradual improvement in the energy efficiency of both buildings, consistent with the renovation works progressively carried out by UCLouvain over the period.

10-year projection. The trend is extrapolated over a 10-year horizon (2026–2035), aligned with UCLouvain's carbon neutrality target by 2035 [37].

3.2.3 Intervention Scenarios

Four scenarios are modelled. Each applies a multiplicative factor $f(t, s)$ to the baseline consumption predicted by the regression:

$$C_{\text{scenario}}(t) = \hat{C}(t) \times f(t, s) \tag{3.22}$$

Scenario	Factor f	Rationale
Normal	1.0	Baseline: historical trend extended with no additional intervention.
Slowheat	0.5	A 50% reduction in heating consumption through temperature setpoint management, applying a conservative factor relative to the 57% reported in the literature (see Section 2.6). No CAPEX is assumed.
Biomass	0 from 2028	Full replacement of fossil heat from January 2028, upon commissioning of the UCLouvain biomass plant (see Section 2.7).
Progressive Biomass	$\frac{2}{3}$ in 2028, $\frac{1}{3}$ in 2029, 0 from 2030	Conservative scenario accounting for the gradual ramp-up of the plant and progressive building connections.

Table 3.2: Definition of the four scenarios and their reduction factors

3.2.4 Savings Calculation

Energy savings

For each scenario s and year y, energy savings relative to the Normal scenario are computed as:

$$\Delta E_{y,s} = C_{y,\text{Normal}} - C_{y,s} \tag{3.23}$$

where $\Delta E_{y,s}$ is the saved energy, $C_{y,\text{Normal}}$ is the consumption for the actual scenario, also called *Normal*, and $C_{y,s}$ is the consumption for the considered scenario. All quantities are expressed in MWh.

Financial savings

Financial savings $\Delta F_{y,s}$ are derived by multiplying energy savings $\Delta E_{y,s}$ by the natural gas price p_{gas}:

$$\Delta F_{y,s} = \Delta E_{y,s} \times p_{\text{gas}} \tag{3.24}$$

The central value used is $p_{\text{gas}} = 50$ €/MWh (= 0.050 €/kWh), reflecting the recent Belgian market trend in 2026, reported by TotalEnergies Belgium [38].

CO_2 emission reductions

Avoided emissions are estimated using the *Belgian natural gas emission factor*:

$$\Delta \text{CO}_{2,y,s} = \Delta E_{y,s} \times e_{\text{gas}} \tag{3.25}$$

with $e_{gas} = 0.205$ tCO_2/MWh. This value corresponds to the direct combustion emission factor for natural gas in Belgium (tank-to-wheel, excluding upstream extraction and transport) [39].

3.2.5 Financial Analysis

Net Present Value (NPV)

The Net Present Value discounts all future financial flows back to a reference year (2026) to account for the time value of money:

$$\text{NPV} = \sum_{t=0}^{T} \frac{\Delta F_{y_0+t,\,s}}{(1+r)^t} - \text{CAPEX} \tag{3.26}$$

with:

- $r = 4\,\%$: discount rate standard for public-sector projects in Belgium;
- $T = 10$ years (horizon: 2026–2035);
- CAPEX = 0 € for all scenarios: the *Slowheat programme* relies on organizational measures, and the biomass plant CAPEX is borne by GBES under a Power Purchase Agreement (PPA), not directly by UCLouvain [29].

Risk analysis: Monte Carlo simulation

Since the natural gas price is inherently volatile, a probabilistic approach is adopted to quantify financial uncertainty. A Monte Carlo simulation of 5,000 draws models the gas price as a normally distributed random variable:

$$p_{\text{gas}} \sim \mathcal{N}(\mu = 50, \sigma^2 = 17^2) \quad [\text{€/ MWh}] \tag{3.27}$$

where $\mu = 50$ €/MWh is the central market price and $\sigma = 17$ €/MWh is calibrated on observed Belgian price volatility (2018–2024), representing a relative volatility of approximately 33%. Prices are clipped to the physical range [10, 300] €/MWh. For each draw, cumulative gross savings and NPV are recomputed for each scenario. This yields a full distribution of financial outcomes, summarized by the 5th, 50th, and 95th percentiles (P5, P50, P95).

ETS-2 carbon pricing

From 2028 onwards, the EU Emissions Trading System for buildings (ETS-2) will impose a carbon surcharge on natural gas consumption. The surcharge is modelled as an addition to the base gas price:

$$p_{\text{eff}}(y) = \begin{cases} p_{\text{gas}} & \text{if } y < 2028 \\ p_{\text{gas}} + p_{\text{ETS2}} \times e_{\text{gas}} & \text{if } y \geq 2028 \end{cases} \tag{3.28}$$

where p_{ETS2} is the ETS-2 carbon price and $e_{\text{gas}} = 0.205$ tCO_2/MWh. Three ETS-2 price scenarios are considered: 45, 55, and 65 €/tCO_2, based on the European Commission's low, central, and high estimates for 2028–2030.

Reference: Sart-Tilman campus (ULiège)

The CO_2 savings are contextualized using the biomass cogeneration plant of ULiège's Sart-Tilman campus as a regional benchmark. That installation produces 42,378 MWh of heat per year, covering 70% of campus thermal needs, implying total campus thermal demand of approximately 60,540 MWh/year (= 42,378 / 0.70). It achieves a reported CO_2 reduction of 5,200 tCO_2/year (carbon balance method) [40]. The expected reduction for each building is scaled proportionally:

$$\Delta CO_{2,\text{ref}} = 5{,}200 \times \frac{\bar{C}_{\text{Normal}}}{60{,}540} \quad [tCO_2/\text{year}] \tag{3.29}$$

where $\bar{C}_{\text{Normal}}$ is the average annual Normal consumption of the building considered.

3.2.6 Software and implementation

The entire analysis was implemented in Python, using the libraries `pandas` for data manipulation and time-series handling, `numpy` for numerical operations and Monte Carlo random sampling, `scikit-learn` for linear regression and model evaluation, and `matplotlib` to plot figures. Results are thus presented through figures generated directly from the code.

Chapter 4

Results and Analysis

4.1 Remaining potential and economic analysis of further renovations

4.1.1 Trends in standardized consumption from 2017 to 2025

The analysis of climate-normalized energy consumption shows a significant and continuous improvement in both buildings. Figure 4.1 highlights the evolution of the specific heating consumption between 2017 and 2025.

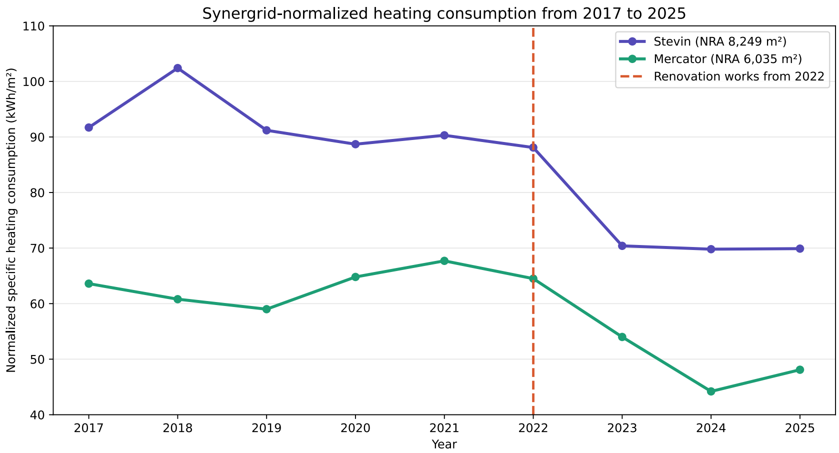

Figure 4.1: Evolution of climate-normalized specific heating consumption for Stevin and Mercator

Between 2017 and 2025, the specific consumption decreases by 23.8% for Stevin, from 91.7 to 69.9 kWh/m^2, and by 24.4% for Mercator, from 63.6 to 48.1 kWh/m^2. The main change appears between 2022 and 2023, corresponding to the insulation works carried out during this period and the renovation of wing A of the Stevin building. Before this period, yearly variations remain limited to around ±5%, more likely linked to occupancy conditions than to structural changes. All detailed data can be found in Appendix B.

Overall heat loss coefficient K and U_{global}

The K coefficient and its equivalent U_{global}, shown in Figure 4.2, confirm the same trend: the lower the U_{global} value, the lower the heat losses through the building envelope and therefore the lower the heating demand.

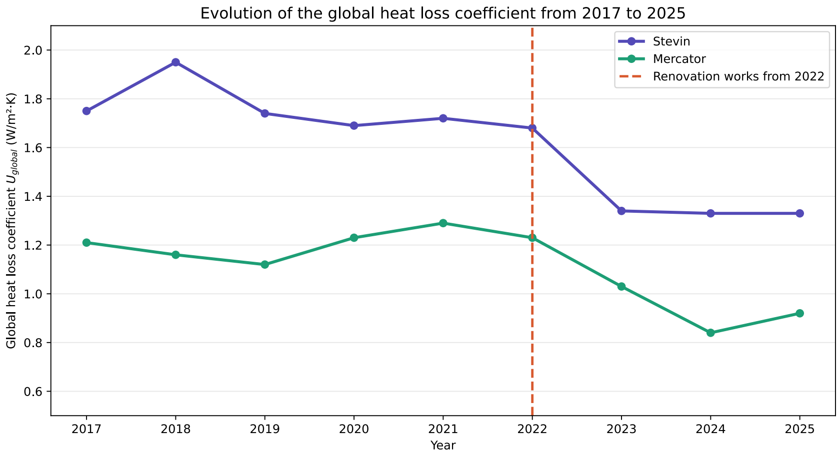

Figure 4.2: Evolution of climate-normalized specific heating consumption for Stevin and Mercator

The results show a clear improvement after the renovation works: for Stevin, the average U_{global} decreases from 1.75 to 1.33 W/m^{2}K (−24.0%), and for Mercator from 1.21 to 0.93 W/m^{2}K (−23.2%). The full set of annual values can be found in Table B.2 in Appendix B. The intra-period stability of K values further supports the reliability of the method, confirming that the coefficient captures the intrinsic thermal characteristics of the buildings independently of weather conditions.

4.1.2 Energy performance of the buildings

The energy signature provides a more detailed thermal characterization of the buildings, complementing the annual K coefficient approach. The regression parameters are summarized in Table 4.1, and the graphical comparison between pre- and post-renovation periods is shown in Figures 4.3a and 4.3b.

Three main observations can be made. First, the slope decreases by 19.3% for Stevin and 19.6% for Mercator, reflecting a reduced sensitivity of both buildings to outdoor temperature and therefore lower heat losses, visible in the figures as less steep post-renovation regression lines.

Building	**Period**	**Slope** a	**Intercept** b	R^2	T_{nc} **(°C)**	H_{eq} **(W/m^{2}K)**
Stevin	2017–2022	−1.275	20.15	0.882	15.8	1.75
Stevin	2023–2025	−1.029	16.33	0.858	15.9	1.41
Mercator	2017–2022	−0.812	13.24	0.879	16.3	1.11
Mercator	2023–2025	−0.653	10.81	0.856	16.6	0.89

Table 4.1: Energy signature parameters before and after the renovation works

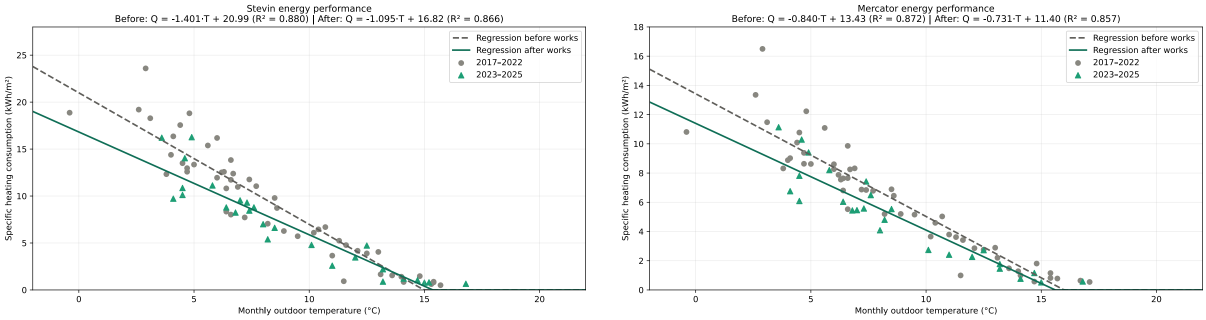

(a) Energy signature of the Stevin building

(b) Energy signature of the Mercator building

Figure 4.3: Comparison of the energy signatures before and after the renovation works for Stevin and Mercator

Second, the intercept b also decreases, by about 19% for Stevin and 18% for Mercator, as reported in Table 4.1, indicating a reduction in more permanent losses such as internal distribution losses, auxiliaries, or remaining infiltration, typical of an envelope renovation. Graphically, this appears as a downward shift of the post-renovation regression line.

Third, the non-heating temperature T_{nc} remains almost unchanged (from 15.8 to 15.9°C for Stevin and from 16.3 to 16.6°C for Mercator, as reported in Table 4.1), suggesting that the setpoint temperature and operating mode did not change significantly. The observed reduction is therefore attributable to the renovation works themselves rather than to behavioural changes.

Finally, the results are consistent with the U_{global} values obtained previously: H_{eq} = 1.41 vs U_{global} = 1.33 W/m^{2}K for Stevin (6% difference) and 0.89 vs 0.93 W/m^{2}K for Mercator (4% difference), reinforcing the reliability of both approaches. The R^2 remains stable, from 0.882 to 0.858, which is consistent with a passive envelope renovation that preserves the thermal coupling structure. The absolute RMSE decreases from 2.06 to 1.70 kWh/m^2, corresponding to a reduction of 17.8%, confirming a more homogeneous post-renovation thermal behaviour.

4.1.3 Analysis of monthly residues

The residual analysis relies on three complementary representations. First, monthly bar plots compare post-renovation consumption with the pre-renovation reference signature. Second, yearly residual curves show the evolution of this difference for each post-renovation year. Finally, seasonal residual patterns compare each month with the yearly energy signature of the same year, to identify recurring operational or seasonal effects.

Residuals relative to the pre-renovation reference signature

Figure 4.4 shows the monthly residuals for 2023-2025[1]. Negative residuals correspond to savings compared with the pre-renovation reference signature, while positive residuals correspond to overconsumption. The results are mainly negative for both buildings, which confirms that the post-renovation consumption is generally lower than the level predicted by the 2017–2022 reference signature.

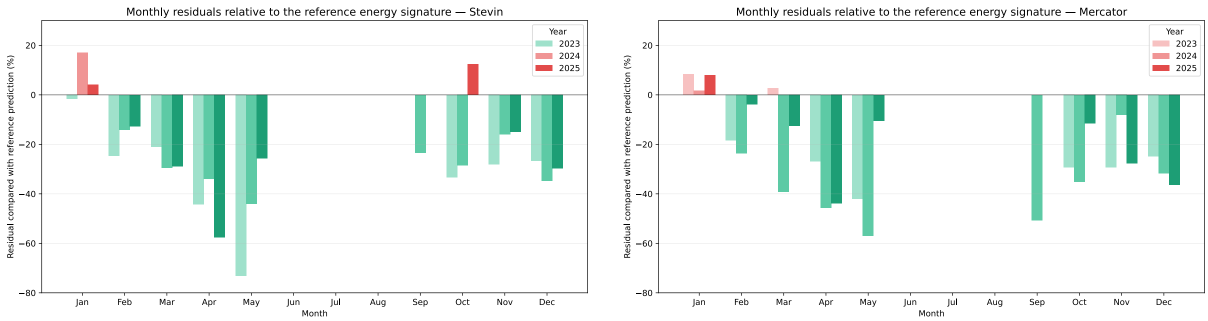

(a) Stevin

(b) Mercator

Figure 4.4: Monthly residuals relative to the pre-renovation reference energy signature

The annual aggregated savings are summarized in Table 4.2. On average, the reduction reaches 20.5% for Stevin and 19.1% for Mercator. The two values are close, which supports the consistency of the renovation effect observed on both buildings. The few positive residuals are mainly concentrated in January, most likely due to the post-holiday recovery, and, for Stevin, partly in October. These local overconsumptions do not change the global trend, but they suggest specific operational effects that are analyzed later.

Year	Stevin	Mercator
2023	−25.6%	−16.0%
2024	−18.6%	−25.2%
2025	−17.3%	−16.2%
Average	−20.5%	−19.1%

Table 4.2: Annual aggregated savings relative to the pre-renovation reference signature.

The seasonal distribution of the savings is also visible in Figure 4.4. The strongest relative savings occur during mid-season months, especially from March to May, while the winter months show smaller savings and sometimes positive residuals. This is confirmed by the

[1]The analysis is only based on the heating months, from September to May. The months from June to August are excluded because the heating system is assumed to be off during this period. The remaining consumption, such as DHW or auxiliaries, is no longer mainly temperature-dependent, so the linear signature $Q = a \cdot T + b$ loses its physical meaning.

temperature-bin analysis in Table 4.3. For outdoor temperatures between 8 and 16°C, the savings reach approximately 30 to 40%, whereas they become very small, or even slightly positive, below 4°C.

Outdoor temperature range	Stevin	Mercator	Number of months
$T_{\text{ext}} < 4$°C	+4%	+8%	14
4–8°C	−18%	−18%	13
8–12°C	−39%	−33%	5
12–16°C	−31%	−34%	6

Table 4.3: Savings by outdoor temperature range for the post-renovation period 2023–2025.

This seasonal pattern can be explained by two complementary effects. First, there is an algebraic effect: the renovation reduces the slope of the energy signature by about 19%, which means that the absolute reduction in consumption is relatively stable, but represents a larger share of the total demand when the reference consumption is low. Second, there is a physical effect: during mid-season, internal and solar gains cover a larger part of the residual heating demand, which amplifies the apparent relative impact of the insulation. In deep winter, the heating demand remains dominant, and the January operational bias is enough to reduce or even cancel the relative savings.

Yearly residual trajectories

Figure 4.5 compares the three post-renovation years on the same monthly axis. The three curves remain mostly in the same negative range, which indicates that the renovation effect appears immediately after the works and remains visible in 2024 and 2025.

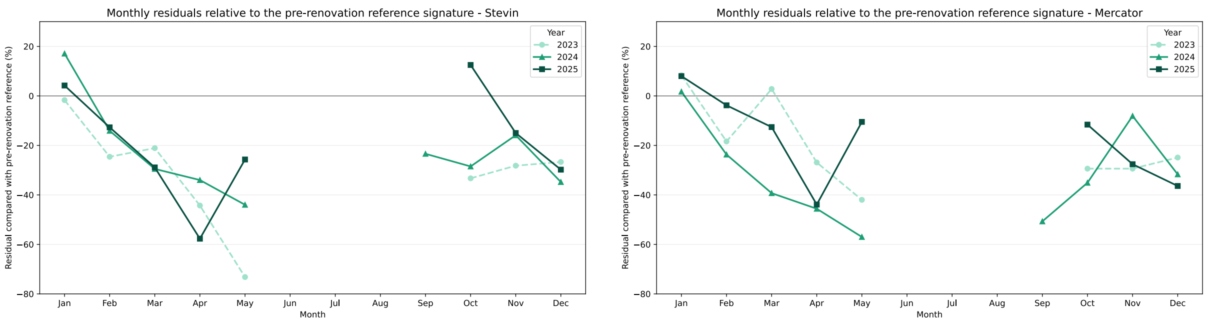

(a) Stevin

(b) Mercator

Figure 4.5: Monthly residual curves relative to the pre-renovation reference energy signature

For Stevin, the largest savings are observed in 2023 during April and May, with residuals reaching approximately −58% to −74%. In 2024 and 2025, the values remain mostly between −25% and −45% during the same period. For Mercator, 2024 shows stronger reductions in February and

March than the two other post-renovation years, but the interannual variability remains limited. Overall, Figure 4.5 does not show any upward drift after the renovation, which suggests that the gain is maintained over the three post-renovation years. The remaining variability, typically around ±15 percentage points for a given month, is mainly linked to differences in weather conditions and building operation.

Seasonal residual pattern relative to the yearly signature

The third representation changes the reference. Instead of comparing each month with the pre-renovation signature, Figure 4.6 compares each month with the yearly energy signature of its own year. This removes the global renovation effect and highlights the residual seasonal pattern. If a yearly linear regression fully described the heating behaviour, these residuals would be close to zero. However, Table 4.4 and Figure 4.6 show that some systematic deviations remain.

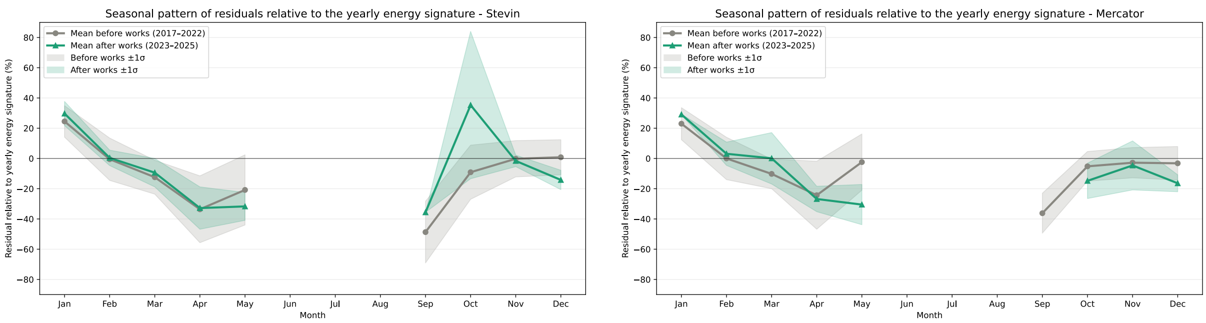

(a) Stevin.

(b) Mercator.

Figure 4.6: Seasonal residual pattern relative to each yearly energy signature, with $\pm 1\sigma$ dispersion bands.

Month	Stevin before	Stevin after	Mercator before	Mercator after
January	+24.5%	+29.7%	+23.0%	+29.1%
February	−0.5%	+0.4%	0.0%	+3.1%
March	−12.4%	−9.4%	−10.2%	+0.1%
April	−33.6%	−32.8%	−24.3%	−26.8%
May	−20.8%	−31.7%	−2.4%	−30.5%
November	−0.2%	−1.6%	−2.8%	−4.6%
December	+0.8%	−14.2%	−3.2%	−16.4%

Table 4.4: Average seasonal residuals relative to the yearly energy signature.

Three main observations can be made. First, the positive January residual is systematic for both buildings and both periods, with values around +23% to +30% in Table 4.4. This effect is also

clearly visible in Figure 4.6. It is probably linked to heating restart after the end-of-year holidays, the building thermal mass is colder, the setpoint is reached again quickly, and the measured consumption exceeds the value predicted by a monthly linear model. Since this bias exists before and after the renovation, it is more likely related to operation than to the envelope.
Second, a negative mid-season residual is observed in April and May. This pattern appears before and after the works and is therefore not only a renovation effect. It rather reflects a structural limitation of the linear energy signature model: during mid-season, free gains cover a larger share of the heating needs than what is captured by a simple regression based on outdoor temperature.
Finally, Figure 4.6 shows that the post-renovation dispersion bands are generally narrower during the main heating months. For Stevin, for example, the standard deviation decreases from 14.0% to 5.1% in February, from 22.1% to 14.0% in April, and from 23.2% to 9.2% in May. This lower dispersion suggests a more homogeneous and predictable thermal behaviour after the works, which is consistent with the expected effect of envelope insulation. The main exception is October for Stevin, where the post-renovation dispersion increases strongly. This is an abnormal monthly behaviour that should be investigated, but it does not modify the annual conclusion.

4.1.4 Cogeneration, primary energy factor and PEB classification

The allocation of gas consumption between the heat and electricity outputs of the cogeneration unit is a methodological choice that directly affects the primary energy factor f_p assigned to the delivered heat. Three allocation methods are compared in Table 4.5, together with the resulting f_p of the cogenerated heat and the average f_p of the district heating network, assuming a cogeneration share of 30% in 2025.

Method	Formula	$f_{p,\text{cogen}}$	$f_{p,\text{network}}$
Default	$f_p = 1.0$	1.000	1.078
PER	$f_p = 1/(\eta_{\text{th}} + \eta_e)$	1.391	1.195
Substitution	$f_p = 1/\eta_{\text{th}} - (\eta_e/\eta_{\text{th}})\, f_{p,\text{elec}}$	0.506	0.930

Table 4.5: Comparison of primary energy factor allocation methods for cogenerated heat.

The difference between the three methods, from 0.930 to 1.195 for the network factor, is the main uncertainty source for the calculation of the specific primary energy consumption E_{spec}.

Specific primary energy consumption and approximate E_w

For Stevin SC04, the 2025 values used are a heating consumption of 520.0 MWh, an estimated electricity consumption of 165 MWh, and a heated floor area of 6 427 m^2. The resulting values are given in Table 4.6.

Method	$f_{p,\text{network}}$	E_{heat} (MWh_{pe})	E_{elec} (MWh_{pe})	E_{spec} ($\text{kWh}_{\text{pe}}/\text{m}^2$)	E_w
Default	1.078	560	412	151	80
PER	1.195	621	412	161	85
Substitution	0.930	483	412	139	74

Table 4.6: Specific primary energy consumption and approximate E_w for Stevin SC04 in 2025.

For Mercator SC10, the 2025 values used are a heating consumption of 261.6 MWh, an estimated electricity consumption of 121 MWh, and a heated floor area of 5 458 m^2. The results are shown in Table 4.7.

Method	$f_{p,\text{network}}$	E_{heat} (MWh_{pe})	E_{elec} (MWh_{pe})	E_{spec} ($\text{kWh}_{\text{pe}}/\text{m}^2$)	E_w
Default	1.078	282	302	107	57
PER	1.195	313	302	113	60
Substitution	0.930	243	302	100	53

Table 4.7: Specific primary energy consumption and approximate E_w for Mercator SC10 in 2025.

The E_{spec} values vary by about ±10% around the default method. This confirms that the allocation method is a second-order parameter compared with the absolute consumption level, but it is still large enough to move a building close to a PEB class threshold. For Stevin, E_w ranges from 74 to 85, so the building remains in class D whatever the method. The 2023 thermal renovation was therefore not sufficient to reach class C, whose threshold is $E_w \leq 60$. Mercator is much closer to the C–D boundary, with E_w between 53 and 60, and reaches the class C threshold with the default method.

The role of electricity is also important. With the assumption of 20 kWh/m^2 for auxiliary electricity uses, electricity alone represents about 42% of Stevin's E_{spec} and 56% of Mercator's. This means that, especially for Mercator, the thermal envelope is no longer the only limiting factor. Future improvement in the PEB result would therefore also need to target electricity uses.

Regulatory positioning and evolution from 2017 to 2025

The Walloon PEB classification gives contrasted results for the two buildings. Stevin reaches an E_{spec} between 139 and 161 $\text{kWh}_{\text{pe}}/\text{m}^2$ and an E_w between 74 and 85, which corresponds to class D. It remains above the class C threshold and also clearly above the Q-ZEN target for new buildings, defined by $E_w \leq 45$. Mercator reaches an E_{spec} between 100 and 113 $\text{kWh}_{\text{pe}}/\text{m}^2$ and an E_w between 53 and 60, which places it at the limit between class C and class D. With the

substitution method, it reaches $E_w = 53$, which is closer to the Q-ZEN threshold.
These results are based on the real 2025 consumption, without climate normalization, and include an estimation of electricity consumption. If heating alone is considered, without electricity, the E_w values decrease to 40–51 for Stevin and 24–30 for Mercator. On the thermal criterion alone, Mercator would therefore be positioned around class A–B.
The evolution from 2017 to 2025, calculated on heating only with the default method for comparability, is presented in Table 4.8. It clearly shows the break after the 2023 renovation works.

Year	E_{spec} Stevin (kWh_{pe}/m^2)	Ew Stevin	E_{spec} Mercator (kWh_{pe}/m^2)	Ew Mercator
2017	120	63	72	38
2022	97	51	61	32
2023	81	43	54	29
2024	86	45	47	25
2025	87	46	52	27

Table 4.8: Evolution of heating-only E_{spec} and Ew using the default method.

On the heating-only indicator, Stevin reaches the Q-ZEN threshold in 2023, before increasing slightly in 2024 and 2025 because of residual climatic and operational variability. Mercator remains comfortably below this threshold from 2023 onwards. This confirms that the thermal performance improved strongly after the renovation, but that the complete PEB positioning is now strongly influenced by the electricity component.

Methodological limitations

The results remain approximate because of five main uncertainties. First, the cogeneration allocation method changes E_{spec} by about ±10%, but this is mainly a convention choice rather than a measurement error. Second, Ach is approximated by the NRA, which may induce a proportional error of about 5–10%. Third, electricity is estimated at 20 kWh/m^2, since it represents up to 56% of total E_{spec}, it is the main uncertainty on E_w. Fourth, the cogeneration share is assumed to be 30% for the whole year, although it may vary seasonally. Finally, the E_w calculation remains approximate and does not replace an official PEB simulation. A comparison with non-renovated UCLouvain buildings would be needed to isolate the renovation effect more formally.

4.1.5 Prioritizing investments: what the economic analysis reveals

The comparison of six renovation scenarios, based on Ferrari & Beccali (2017) [4] and Ma et al. (2012) [5], shows a very contrasted economic hierarchy. Operational measures have payback times below five years, whereas envelope renovations are difficult to justify only through a simple return on investment at the current heat price.

Three main conclusions can be drawn from Tables 4.9 and 4.10. First, quick wins are the most robust option. With payback times between roughly 3 and 7 years and break-even prices below 40 EUR/MWh, scenarios S1 and S2 remain profitable under almost all plausible market conditions. They should therefore be implemented independently of any long-term renovation strategy, because they are the only measures that are clearly defensible on a purely economic basis at the current energy price.

Scenario	Reduction in Q	Investment (kEUR)	Savings (EUR/year)	Verdict
S1 - Operational quick wins	7.5%	14	3 590	No regret
S2 - Technical quick wins	20%	52	9 575	No regret
S3 - Standard envelope (DGR)	20%	1 992	9 575	Not profitable alone
S4 - Reinforced envelope (DGR-30)	22%	2 131	10 533	Decreasing returns
S5 - Ambitious envelope (DGR-50)	26%	2 271	12 448	Penalizing over-insulation
S6 - Global renovation	45%	2 724	21 543	Decarbonization logic

Table 4.9: Comparative summary of the six renovation scenarios for Stevin and Mercator combined.

Scenario	Stevin (EUR/MWh)	Mercator (EUR/MWh)	Interpretation
S1 - Operational quick wins	19	27	Always reached since 2021
S2 - Technical quick wins	26	37	Reached since 2022
S3 to S5 - Envelope renovation	869–1 444	1 266–1 444	Outside market range
S6 - Global renovation	581	918	Only reachable in a long crisis scenario

Table 4.10: Break-even heat price for a 10-year payback.

Second, envelope over-insulation shows decreasing returns. Moving from S3 to S5 only adds 6 percentage points of consumption reduction, while increasing the investment by about 160 kEUR per building, without a real improvement in ROI. This is consistent with the results of Ferrari & Beccali (2017) and suggests that the insulation ambition should be moderated in favour of a more systemic approach. The limitation is not technical but economic: windows alone represent around 80% of the envelope cost, which strongly limits the profitability of heavy envelope renovation. Finally, the global renovation scenario remains the most effective in absolute terms, with a 45% reduction in heat demand. However, its payback time is longer than one century, so it cannot be justified only through a simple ROI logic. Its relevance rather comes from other criteria, such as EPBD 2030 compliance, decarbonization, extension of the building lifetime, heritage value and indoor comfort. This shift from economic profitability to strategic decision-making is therefore central for the next part of the analysis.

4.2 Energy and Financial Performance of Intervention Scenarios

This section presents the results of heating consumption savings, energy savings, CO_2 reductions and a financial analysis, depending on the different scenarios that UCLouvain could implement. As a reminder, three scenarios were considered: Slowheat, biomass with an immediate effect, and biomass with a progressive effect.

4.2.1 Historical Consumption (2017–2025)

Both buildings exhibit a clear downward trend over the observation period, as summarized in Table 4.11. Stevin decreases from 714 MWh in 2017 to 520 MWh in 2025 (−27%), while Mercator drops from 362 MWh to 262 MWh (−28%), consistent with the incremental renovation works carried out over the period.

Building	**Mean 2017–2025 (MWh/yr)**	**Min (MWh)**	**Year**	**Max (MWh)**	**Year**
Stevin	611	486	2023	732	2018
Mercator	308	237	2024	395	2021
Combined	**919**	–	–	–	–

Table 4.11: Annual heating consumption – historical data (MWh/year)

The complete monthly heating consumption data for both buildings over the period 2017–2025 are reported in Appendix C.

4.2.2 Predicted Consumption by Scenario

Figures 4.7 and 4.8 present the predicted monthly time series and annual aggregates for the four scenarios over the 10-year horizon. The predictions were calculated as described in Section 3.2.2.

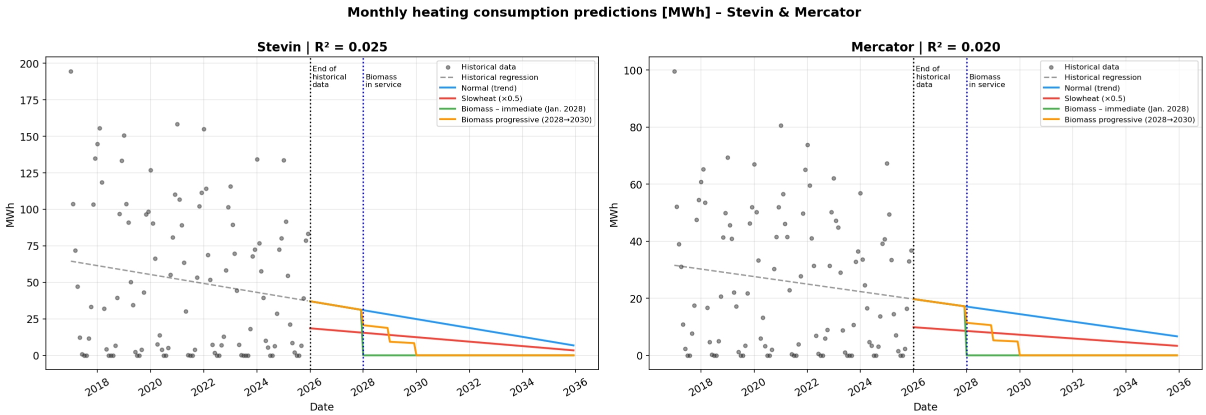

Figure 4.7: Monthly heating consumption predictions for Stevin & Mercator buildings the four scenarios over 10 years. The dashed vertical line marks the biomass plant commissioning date (January 2028).

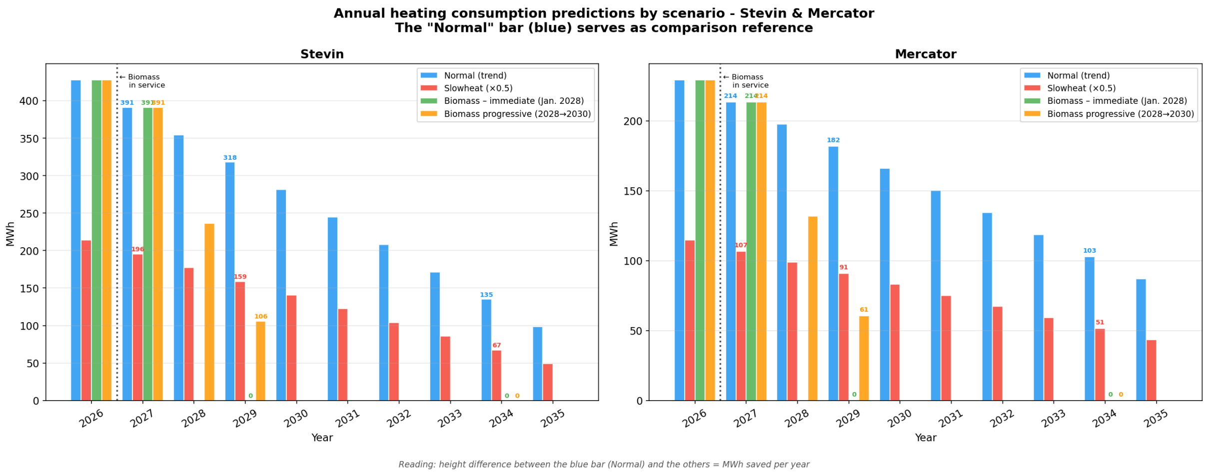

Figure 4.8: Annual predicted consumption by scenario for Stevin & Mercator buildings. The blue bar (Normal) serves as the reference; the height difference with the other scenarios represents the annual savings in MWh.

4.2.3 Energy Savings and CO_2 Reductions

Figure 4.9 shows the annual energy savings for the Stevin & Mecractor buildings. Both the upper plots show the savings for the *Slowheat* scenario for each building. The two lower plots show the savings for the *Immadiate* and *Progressive* Biomass scenarios.
Figure 4.10 shows the annual CO_2 avoided for each building and each scenario.

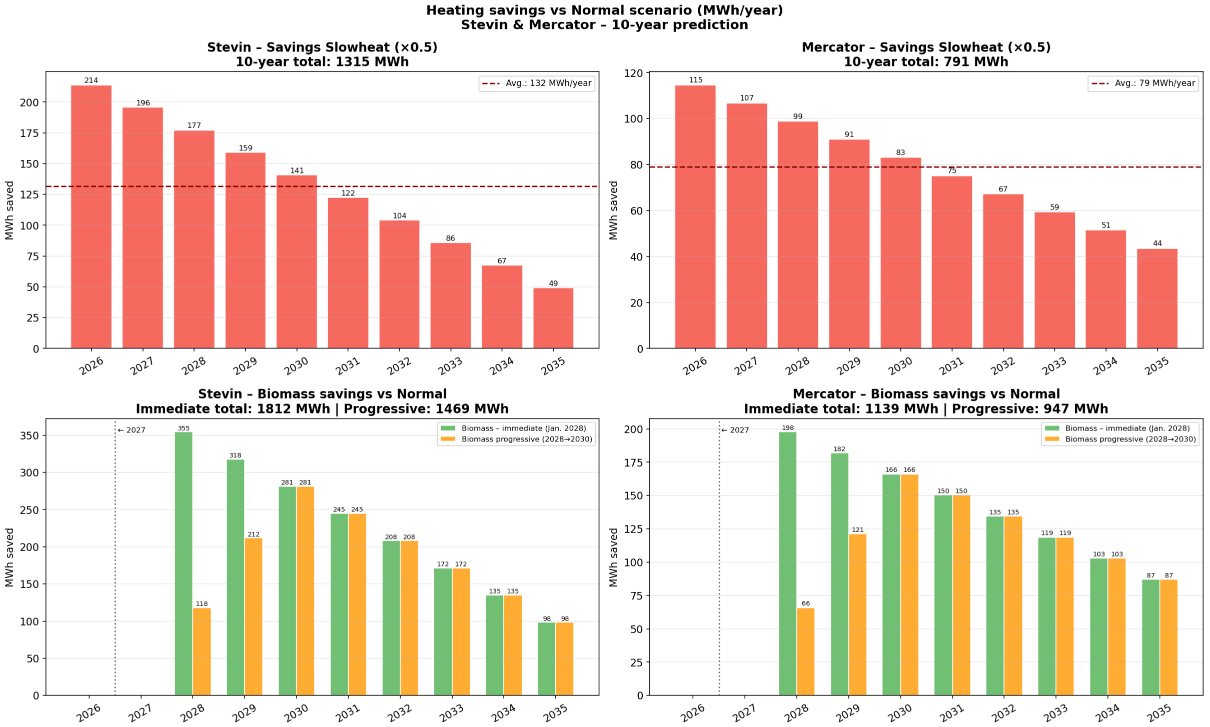

Figure 4.9: Annual energy savings relative to the Normal scenario (MWh/year). Top row: Slowheat scenario; bottom row: comparison of both Biomass scenarios.

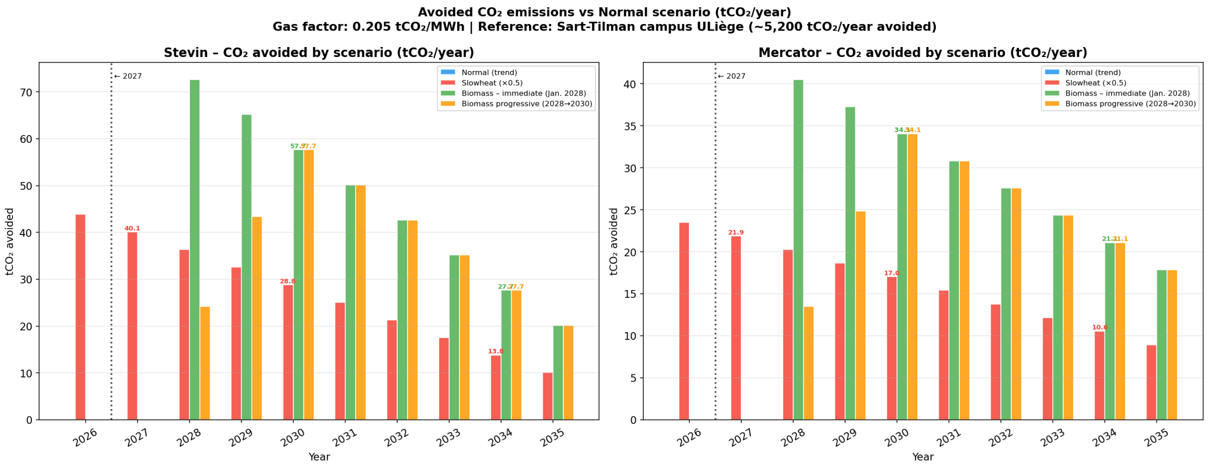

Figure 4.10: Annual CO_2 avoided by scenario (tCO_2/year).

Table 4.12 summarizes the cumulative energy savings and CO_2 reductions over 10 years for each scenario and building.

Building	Scenario	Energy savings (MWh)	CO_2 avoided (t)
Stevin	Slowheat	1,315	265.7
	Biomass (immediate)	1,812	365.9
	Biomass (progressive)	1,469	296.8
Mercator	Slowheat	791	159.8
	Biomass (immediate)	1,139	230.2
	Biomass (progressive)	947	191.3

Table 4.12: Cumulative energy savings and CO_2 reductions over 10 years by scenario and building (CO_2 factor: 0.202 tCO_2/MWh)

The immediate Biomass scenario yields the highest total energy savings (2,951 MWh combined), followed by Progressive Biomass (2,416 MWh) and Slowheat (2,106 MWh). This ranking holds consistently for both buildings individually: for Stevin, the immediate Biomass scenario saves 1,812 MWh against 1,315 MWh for Slowheat; for Mercator, 1,139 MWh against 791 MWh. The stronger performance of the Biomass scenarios over this horizon reflects the fact that, from 2028 onwards, fossil consumption is eliminated entirely, generating larger annual savings than the Slowheat's continuous but partial (50%) reduction.

4.2.4 Financial Analysis

Net Present Value and Gross Savings

Figure 4.11 and Figure 4.12 present the cumulative NPV by scenario and the discounted annual financial savings respectively.
Figures 4.11 and 4.12 provide complementary perspectives on the financial performance of each scenario. The cumulative NPV curves (Figure 4.11) reveal a clear crossover effect: the Slowheat scenario accumulates savings steadily from 2026, while both Biomass scenarios start from zero and only diverge upward from 2028 onwards. For Stevin, the immediate Biomass scenario reaches a total NPV of 75,731 €, outperforming Slowheat (57,962 €) and progressive Biomass (60,095 €). The same ranking holds for Mercator, with respective NPVs of 47,156 €, 34,444 €, and 38,268 €. Notably, the progressive Biomass curve crosses above the Slowheat curve around 2032 for both buildings, confirming that even a gradual transition to biomass becomes financially superior in the medium term.

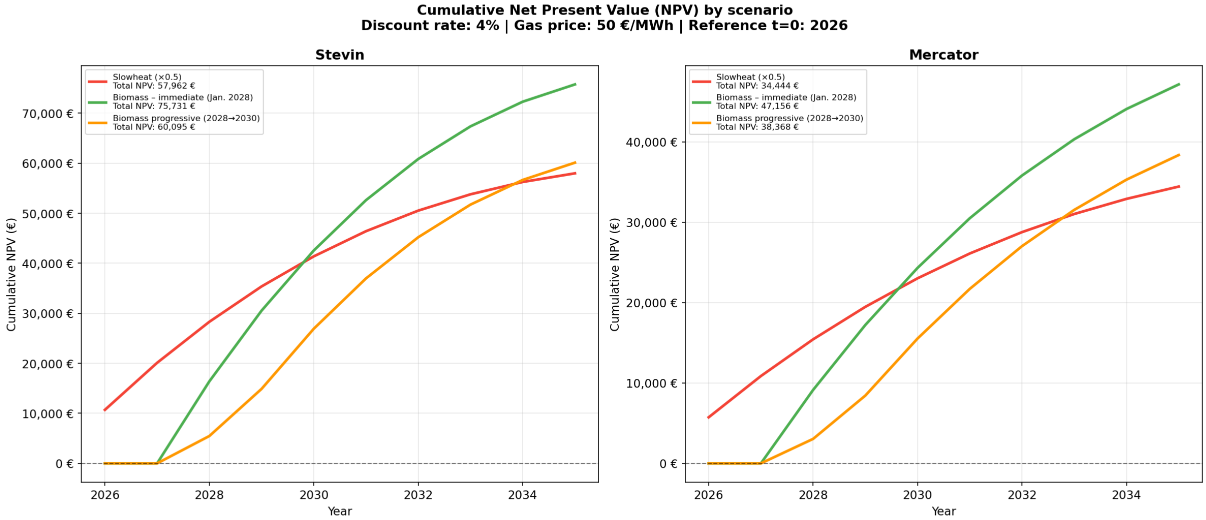

Figure 4.11: Cumulative NPV by scenario (discount rate: 4%). The vertical axis represents the present value of savings accumulated since 2026.

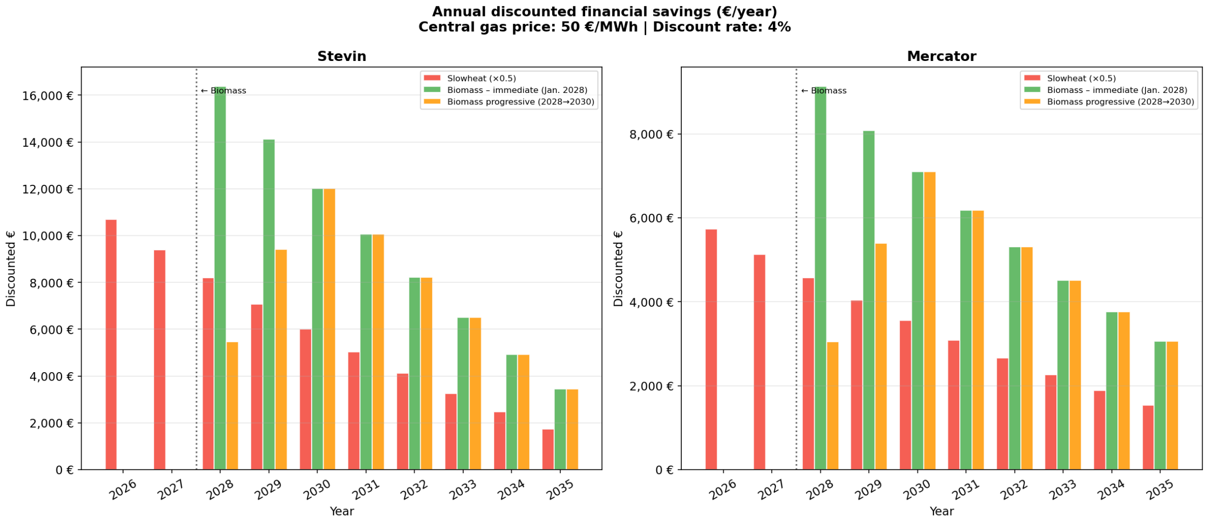

Figure 4.12: Discounted annual financial savings (€/year). Values decrease slightly over time due to the 4% discount rate.

Risk Analysis

ETS-2 carbon pricing. From 2028 onwards, the EU ETS-2 mechanism will impose a carbon surcharge on natural gas consumption in buildings. Using the European Commission's central estimate of 55 €/tCO_2, this adds approximately 11 €/MWh to the effective gas price. As shown in Figure 4.13 and Table 4.13, this further improves the relative performance of the Biomass scenarios, which eliminate fossil consumption exactly when the surcharge becomes active: the immediate Biomass gross savings increase from 147,550 € (no ETS-2) to 174,375 € (+18%), while Slowheat gains only +13%.

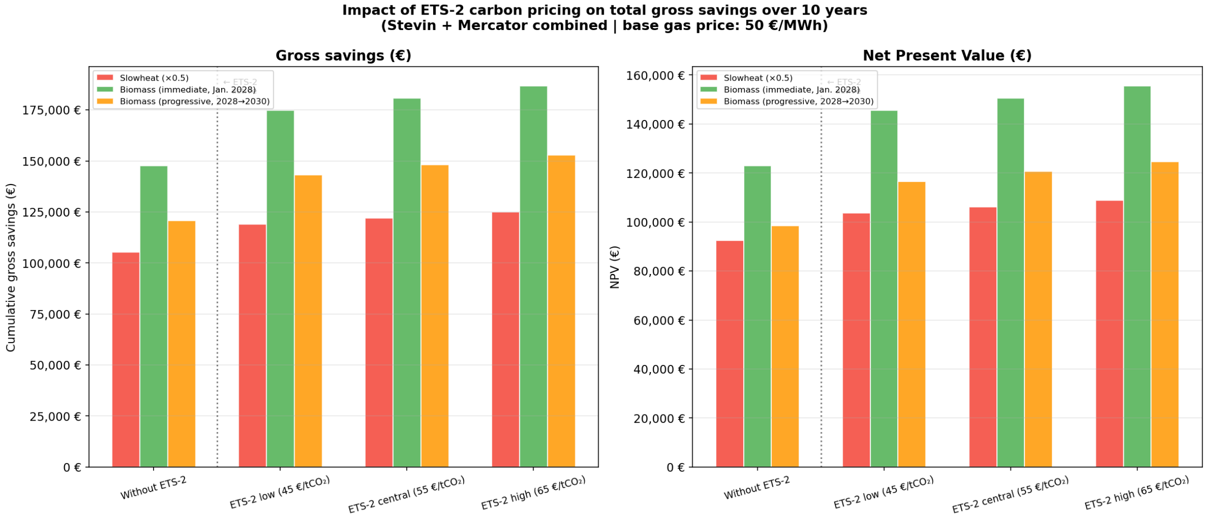

Figure 4.13: Impact of ETS-2 carbon pricing on gross savings and NPV over 10 years (Stevin + Mercator combined; base gas price: 50 €/MWh).

Scenario	**No ETS-2**	**Low (45 €)**	**Central (55 €)**	**High (65 €)**
Slowheat	105,319	118,732	121,713	124,693
Biomass (immediate)	147,550	174,375	180,336	186,297
Biomass (progressive)	120,812	142,776	147,656	152,537

Table 4.13: Gross savings (€, over 10 years) under different ETS-2 carbon prices [€/tCO_2]

Monte Carlo simulation. As explained in Section 3.2.5, a Monte Carlo simulation is used to used to quantify the financial uncertainty of the gas price. Each used variable for the simulation is described in Section 3.2.5. The results are illustrated in Figures 4.14 and 4.15 and summarized in Table 4.14. The immediate Biomass scenario dominates across all percentiles. Even in the pessimistic tail (P5, corresponding to a gas price of approximately 35 €/MWh), it generates 102,279 €, above the P5 of both other scenarios. At the median (P50), its savings of 222,318 € exceed those of Slowheat (158,687 €) and Progressive Biomass (182,031 €). The cumulative distribution functions in Figure 4.15 confirm this dominance: for any given savings threshold, the immediate Biomass curve has the highest probability of exceeding it.

Scenario	**P5 (€)**	**P50 (€)**	**P95 (€)**
Slowheat	47,537	105,801	164,045
Biomass (immediate)	66,599	148,225	229,824
Biomass (progressive)	54,530	121,365	188,177

Table 4.14: Monte Carlo results: gross savings distribution over 10 years (5,000 simulations, gas price $\sim \mathcal{N}(50, 17)$ €/MWh)

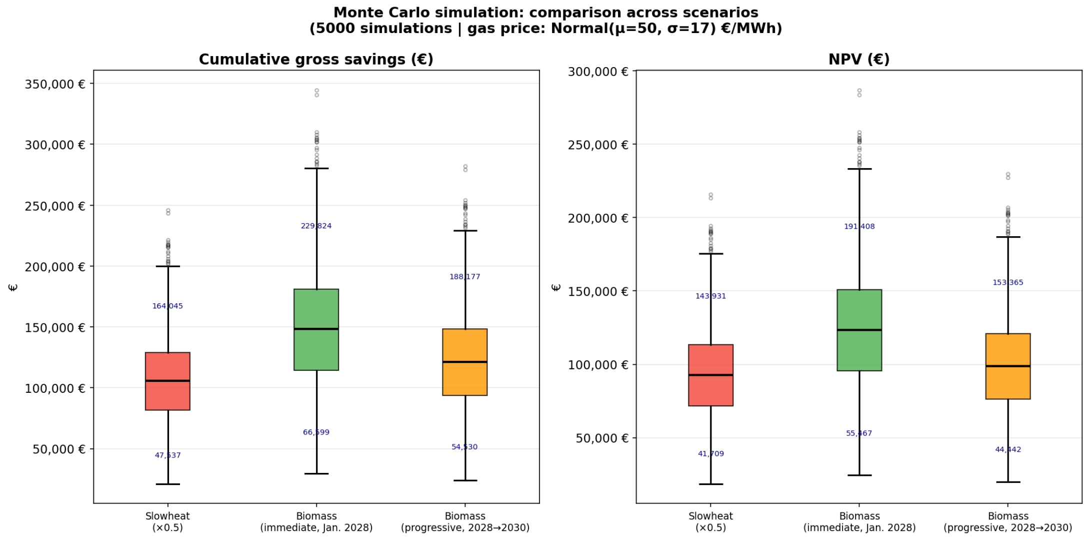

Figure 4.14: Monte Carlo simulation: box plots of gross savings and NPV distributions across scenarios (5,000 simulations). P5 and P95 values are annotated above and below each box.

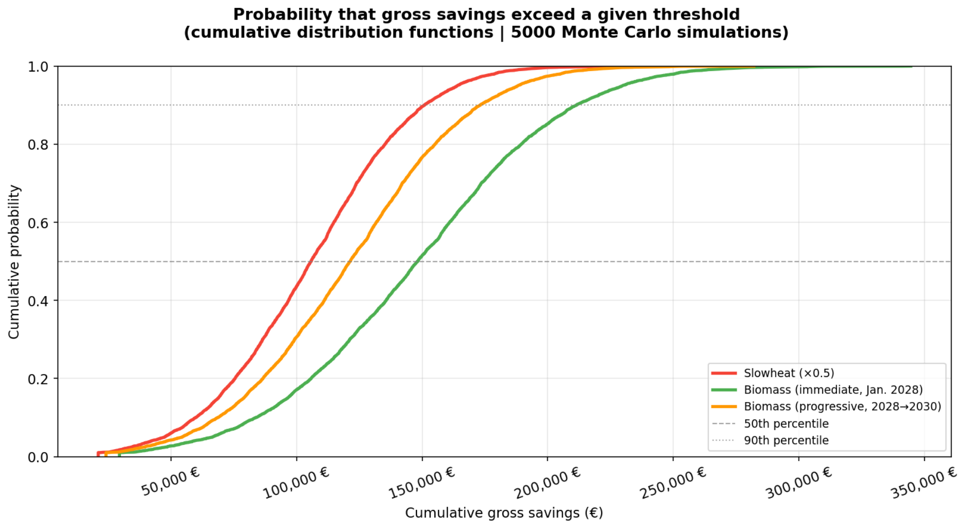

Figure 4.15: Monte Carlo simulation: cumulative distribution functions of gross savings.

4.3 Limitations

The results presented in this chapter are subject to several limitations.

4.3.1 Limitations of the energy performance characterization

1. **Surface area approximation**: the NRA approximates the heated area A_{ch} with an estimated discrepancy between 5 and 10%, introducing a systematic uncertainty in specific consumption figures and PEB results.

2. **Stationary model**: the energy signature and K coefficient do not capture thermal inertia, dynamic solar gains, or transient effects, unlike more complex ARX or RC models.

3. **PEB comparison by analogy**: the E_{spec} and E_w values are indicative estimates that do not replace an official PEB audit.

4. **Cogeneration efficiency**: the primary energy factor is estimated from only six months of data (January–June 2025), which may not be representative of annual operation.

5. **2020 outlier**: the Covid-19 campus closure artificially suppressed consumption in 2020, amplifying the downward trend in both the normalized analysis and the regression.

4.3.2 Limitations of the scenario modelling and financial analysis

1. **Low R^2 of the regression**: the linear regression captures the long-term consumption trend but remains insensitive to seasonal patterns, with an RMSE of approximately 50 MWh/month for Stevin. Results should therefore be interpreted with caution at the individual year level, and are more meaningful over the full 10-year horizon.

2. **Gas price and Monte Carlo distribution**: the central gas price of 50 €/MWh reflects recent Belgian market conditions but remains an approximation. The Monte Carlo simulation partially addresses this uncertainty, though the normal distribution assumed is symmetric and may underestimate the probability of extreme upside events.

3. **Biomass CAPEX not modelled**: the contractual heat purchase price agreed under the Power Purchase Agreement (PPA) with GBES is not publicly available and is assumed cost-neutral relative to gas, which may overestimate net savings for the biomass scenarios.

4. **ETS-2 price uncertainty**: for simplicity, the ETS-2 carbon price is modelled as a fixed value from 2028 under three scenarios (45, 55 and 65 €/tCO_2). In reality, this price will itself be subject to market fluctuations and potential policy revisions, this a more precise study would require modelling its dynamic evolution over the 2028–2035 period.

5. **Slowheat transposability**: the 50% reduction factor is derived conservatively from residential results, and its actual achievability in a tertiary university building remains uncertain.

Chapter 5

Conclusion

This master thesis's purpose is to answer the following research question: *How can the actual energy performance of the Stevin and Mercator buildings be characterized, and which intervention scenarios would enable UCLouvain to meet its decarbonization targets by 2035?*

To address this question, the work was structured in two complementary parts. The first part characterized the actual thermal behaviour of both buildings through climate-normalized consumption analysis, energy signatures, and residual analysis. The second part modelled three intervention scenarios; Slowheat, immediate Biomass, and progressive Biomass, and evaluated their energy, environmental, and financial performance over a 10-year horizon.

The energy performance characterization reveals a significant improvement in both buildings between 2017 and 2025. Climate-normalized specific consumption decreased by 23.8% for Stevin and 24.4% for Mercator, a reduction driven primarily by the cavity wall insulation works carried out in March 2023. This improvement is confirmed by two independent estimators, the K coefficient and the energy signature slope, which converge to within 4–6%. The stability of the non-heating temperature T_{nc} before and after the renovation further confirms that the observed reduction is attributable to the envelope works rather than to behavioural or operational changes.

However, these improvements remain insufficient to meet UCLouvain's Plan Transition target of zero-carbon buildings by 2035. The PEB analogy places Stevin in class D (Ew $\approx$ 74–85) and Mercator at the C–D boundary (Ew $\approx$ 53–60). What is more, the economic analysis of six renovation scenarios shows that deep envelope renovations cannot be justified on a purely financial basis at current energy prices, with break-even prices ranging from 869 to 1,444 €/MWh for envelope-only scenarios. Quick wins remain the only options that are defensible on a return-on-investment perspective, with payback times below seven years and break-even prices already reached since 2022.

Regarding the intervention scenarios, the immediate Biomass scenario delivers the highest performance across all metrics: cumulative energy savings of 2,951 MWh over 10 years, 596 tCO_2 avoided, and a combined NPV of 122,887 € at the central gas price. The Slowheat scenario, despite requiring no capital expenditure, generates meaningful savings from 2026 onwards (2,106 MWh, NPV of 92,406 €) and represents a valuable short-term complementary measure while the biomass plant is being built. The progressive Biomass scenario offers an intermediate option that accounts for the gradual ramp-up of the plant. The Monte Carlo simulation confirms the robustness of these rankings across all gas price assumptions, and the ETS-2 carbon pricing analysis shows that the financial advantage of the Biomass scenarios will further increase from 2028 onwards, as they eliminate fossil consumption exactly when the carbon surcharge becomes active.

5.1 Perspectives

Several directions could extend this work. On the technical side, integrating heating degree-day normalization directly into the regression model would reduce inter-annual variability, and the actual contractual heat purchase price under the PPA with GBES would allow a more precise assessment of the net financial savings of the Biomass scenarios.

From a managerial perspective, the implementation of Slowheat in a tertiary university setting raises organizational challenges beyond the technical dimension. Achieving a sustained reduction in heating setpoint temperatures requires negotiation with occupants, clear communication on comfort expectations, and the involvement of facility management teams. Future work could explore the governance structures and change management processes needed to roll out such behavioural measures across a large university campus.

From a financial planning perspective, the sensitivity of results to gas price assumptions is a reminder of the importance of integrating energy price risk into UCLouvain's long-term asset management strategy. A more comprehensive lifecycle cost analysis covering maintenance, replacement costs, and residual building value, would provide a stronger basis for investment prioritization, especially in light of the structurally rising carbon costs introduced by ETS-2 from 2028 onwards.

Finally, extending the analysis to the broader UCLouvain campus would allow the development of a prioritization framework for connecting buildings to the district heating network, optimizing capital allocation across a portfolio of buildings with heterogeneous energy profiles.

Bibliography

[1] *Energy Performance of Buildings Directive*. en. URL: https://energy.ec.europa.eu/topics/energy-efficiency/energy-performance-buildings/energy-performance-buildings-directive_en (visited on 05/19/2026).

[2] Anna Carolina Menezes et al. *Predicted vs. actual energy performance of non-domestic buildings: Using post-occupancy evaluation data to reduce the performance gap*. In: *Applied Energy*. Energy Solutions for a Sustainable World - Proceedings of the Third International Conference on Applied Energy, May 16-18, 2011 - Perugia, Italy 97 (Sept. 2012), pp. 355–364. ISSN: 0306-2619. DOI: 10.1016/j.apenergy.2011.11.075. URL: https://www.sciencedirect.com/science/article/pii/S0306261911007811 (visited on 05/27/2026).

[3] Pieter de Wilde. *The gap between predicted and measured energy performance of buildings: A framework for investigation*. In: *Automation in Construction* 41 (May 2014), pp. 40–49. ISSN: 0926-5805. DOI: 10.1016/j.autcon.2014.02.009. URL: https://www.sciencedirect.com/science/article/pii/S092658051400034X (visited on 05/27/2026).

[4] Simone Ferrari and Marco Beccali. *Energy-environmental and cost assessment of a set of strategies for retrofitting a public building toward nearly zero-energy building target*. In: *Sustainable Cities and Society* 32 (July 2017), pp. 226–234. ISSN: 2210-6707. DOI: 10.1016/j.scs.2017.03.010. URL: https://www.sciencedirect.com/science/article/pii/S221067071630659X (visited on 05/27/2026).

[5] Zhenjun Ma et al. *Existing building retrofits: Methodology and state-of-the-art*. In: *Energy and Buildings*. Cool Roofs, Cool Pavements, Cool Cities, and Cool World 55 (Dec. 2012), pp. 889–902. ISSN: 0378-7788. DOI: 10.1016/j.enbuild.2012.08.018. URL: https://www.sciencedirect.com/science/article/pii/S0378778812004227 (visited on 05/27/2026).

[6] Jon Terés-Zubiaga et al. *Cost-effective building renovation at district level combining energy efficiency & renewables – Methodology assessment proposed in IEA EBC Annex 75 and a demonstration case study*. In: *Energy and Buildings* 224 (Oct. 2020), p. 110280. ISSN: 0378-7788. DOI: 10.1016/j.enbuild.2020.110280. URL: https:

//www.sciencedirect.com/science/article/pii/S0378778820310562 (visited on 05/27/2026).

[7] Jeff Haberl, David Claridge, and C. Culp. *ASHRAE's Guideline 14-2002 for Measurement of Energy and Demand Savings: How to Determine What Was Really Saved by the Retrofit*. In: (Jan. 2005).

[8] E. R. Hitchin. *Estimating monthly degree-days*. en. In: *Building Services Engineering Research and Technology* 4.4 (Nov. 1983), pp. 159–162. ISSN: 0143-6244, 1477-0849. DOI: 10.1177/014362448300400404. URL: https://journals.sagepub.com/doi/10.1177/014362448300400404 (visited on 05/26/2026).

[9] *Chauffage des bâtiments et neutralité carbone | Université catholique de Louvain*. fr. URL: https://www.uclouvain.be/fr/universite-transition/chauffage-des-batiments-et-neutralite-carbone (visited on 05/26/2026).

[10] *International Performance Measurement & Verification Protocol*.

[11] Stig Hammarsten. *A critical appraisal of energy-signature models*. en. In: *Applied Energy* 26.2 (1987), pp. 97–110. ISSN: 03062619. DOI: 10.1016/0306-2619(87)90012-2. URL: https://linkinghub.elsevier.com/retrieve/pii/0306261987900122 (visited on 05/26/2026).

[12] Gustav Nordström, Helena Johnsson, and Sofia Lidelöw. "Using the Energy Signature Method to Estimate the Effective U-Value of Buildings". en. In: *Sustainability in Energy and Buildings*. Ed. by Anne Hakansson et al. Vol. 22. Series Title: Smart Innovation, Systems and Technologies. Berlin, Heidelberg: Springer Berlin Heidelberg, 2013, pp. 35–44. ISBN: 978-3-642-36644-4 978-3-642-36645-1. DOI: 10.1007/978-3-642-36645-1_4. URL: https://link.springer.com/10.1007/978-3-642-36645-1_4 (visited on 05/26/2026).

[13] Karl-Erik Westergren, Hans Hogberg, and Urban Norlen. *Monitoring energy consumption in single-family houses*. en. In: ().

[14] A.R. Day and T.G. Karayiannis. *Identification of the uncertainties in degree-day-based energy estimates*. en. In: *Building Services Engineering Research and Technology* 20.4 (Nov. 1999), pp. 165–172. ISSN: 0143-6244, 1477-0849. DOI: 10.1177/014362449902000401. URL: https://journals.sagepub.com/doi/10.1177/014362449902000401 (visited on 05/26/2026).

[15] Henrik Madsen et al. *Reliable building energy performance characterisation based on full scale dynamic measurements*. en. In: ().

[16] Marieline Senave et al. *A simulation exercise to improve building energy performance characterization via on-board monitoring*. en. In: *Energy Procedia* 132 (Oct. 2017), pp. 969–974. ISSN: 18766102. DOI: 10.1016/j.egypro.2017.09.687. URL: https://linkinghub.elsevier.com/retrieve/pii/S1876610217348348 (visited on 05/26/2026).

[17] Marieline Senave. *Characterization of the Heat Loss Coefficient of Residential Buildings Based on In-Use Monitoring Data*. en. In: ().

[18] Chris van Dronkelaar. *QUANTIFYING AND MITIGATING DIFFERENCES BETWEEN PREDICTED AND MEASURED ENERGY USE IN BUILDINGS*. en. In: ().

[19] Stefano Cozza, Jonathan Chambers, and Martin K. Patel. *The Energy Performance Gap in Swiss residential buildings: a roadmap for improvement*. en. In: *Journal of Physics: Conference Series* 2042.1 (Nov. 2021), p. 012143. ISSN: 1742-6588, 1742-6596. DOI: 10.1088/1742-6596/2042/1/012143. URL: https://iopscience.iop.org/article/10.1088/1742-6596/2042/1/012143 (visited on 05/26/2026).

[20] SPW. *Exigences PEB - L'Énergie en Wallonie*. fr. URL: https://energie.wallonie.be/home/performance-energetuique-des-batiments/batiments-residentiels/renovation-walloreno/obligations/exigences-peb.html (visited on 05/27/2026).

[21] D. Majcen, L.C.M. Itard, and H. Visscher. *Theoretical vs. actual energy consumption of labelled dwellings in the Netherlands: Discrepancies and policy implications*. en. In: *Energy Policy* 54 (Mar. 2013), pp. 125–136. ISSN: 03014215. DOI: 10.1016/j.enpol.2012.11.008. URL: https://linkinghub.elsevier.com/retrieve/pii/S0301421512009731 (visited on 05/26/2026).

[22] Dennis Johansson, Hans Bagge, and Åsa Wahlström, eds. *Cold Climate HVAC 2018: Sustainable Buildings in Cold Climates*. en. Springer Proceedings in Energy. Cham: Springer International Publishing, 2019. ISBN: 978-3-030-00661-7 978-3-030-00662-4. DOI: 10.1007/978-3-030-00662-4. URL: http://link.springer.com/10.1007/978-3-030-00662-4 (visited on 05/26/2026).

[23] Geoffrey van Moeseke. *Pour des projets de qualité énergétique*. fr. In: ().

[24] Geoffrey Van Moeseke and Denis De Grave. *Le temps et l'espace de la chaleur: Slowheat.org*. fr. In: *lieuxdits* 24 (Dec. 2023), pp. 22–27. ISSN: 2565-6996, 2294-9046. (Visited on 05/19/2026).

[25] Denis De Grave et al. *Slowheat: chauffer les corps, moins les logements: une recherche collective sur la sobriété de nos pratiques de chauffage*. fr. Ed. by Geoffrey van Moeseke. OCLC: 1572240785. Louvain-la-Neuve, Belgique: PUL, Presses universitaires de Louvain, 2024. ISBN: 978-2-39061-494-4.

[26] *Biomasse : définition, avantages et applications de cette énergie*. fr. Apr. 2011. URL: https://www.connaissancedesenergies.org/fiche-pedagogique/biomasse (visited on 05/19/2026).

[27] R. García et al. *Pelletization of wood and alternative residual biomass blends for producing industrial quality pellets*. en. In: *Fuel* 251 (Sept. 2019), pp. 739–753. ISSN: 00162361. DOI: 10.1016/j.fuel.2019.03.141. URL: https://linkinghub.elsevier.com/retrieve/pii/S0016236119305241 (visited on 05/19/2026).

[28] *Une centrale biomasse pour un avenir neutre en carbone : l'UCLouvain montre la voie | Valbiom - Valorisation de la biomasse*. fr. URL: https://www.valbiom.be/actualites/une-centrale-biomasse-pour-un-avenir-neutre-en-carbone-uclouvain-montre-la-voie (visited on 05/19/2026).

[29] *Une centrale biomasse d'envergure pour alimenter l'UCLouvain en chaleur et électricité vertes | Université catholique de Louvain*. fr. URL: https://www.uclouvain.be/fr/news/une-centrale-biomasse-d-envergure-pour-alimenter-l-uclouvain-en-chaleur-et-electricite-vertes (visited on 05/19/2026).

[30] Jonathan Berk 1962-.... *Corporate finance*. eng. Ed. by Peter DeMarzo 19..-.... 5th ed., global ed. Harlow: Pearson, 2020. ISBN: 978-1-292-30415-1. URL: https://ils.bib.uclouvain.be/global/documents/2056167.

[31] Sergio Copiello, Laura Gabrielli, and Pietro Bonifaci. *Evaluation of energy retrofit in buildings under conditions of uncertainty: The prominence of the discount rate*. en. In: *Energy* 137 (Oct. 2017), pp. 104–117. ISSN: 03605442. DOI: 10.1016/j.energy.2017.06.159. URL: https://linkinghub.elsevier.com/retrieve/pii/S0360544217311179 (visited on 05/26/2026).

[32] Robert L. Harrison, Carlos Granja, and Claude Leroy. *Introduction to Monte Carlo Simulation*. en. In: Bratislava (Slovakia), 2010, pp. 17–21. DOI: 10.1063/1.3295638. URL: https://pubs.aip.org/aip/acp/article/1204/1/17-21/866186 (visited on 05/25/2026).

[33] Jean-Charles Walter and Gerard Barkema. *An introduction to Monte Carlo methods*. en. In: *Physica A: Statistical Mechanics and its Applications* 418 (Jan. 2015). arXiv:1404.0209 [cond-mat.stat-mech], pp. 78–87. ISSN: 03784371. DOI: 10.1016/j.physa.2014.06.014. URL: http://arxiv.org/abs/1404.0209 (visited on 05/25/2026).

[34] *ETS2: buildings, road transport and additional sectors - Climate Action*. en. URL: https://climate.ec.europa.eu/eu-action/carbon-markets/ets2-buildings-road-transport-and-additional-sectors_en (visited on 05/25/2026).

[35] *Degrés-jours - Synergrid*. URL: https://www.synergrid.be/fr/centre-de-documentation/statistiques-et-donnees/degres-jours (visited on 05/27/2026).

[36] Antoine Tilmans et al. *Édition 2015| Résidentiel Bureaux-Services-Enseignement Industriel Autre*. fr. In: ().

[37] *Vers la neutralité carbone en 2035 | Université catholique de Louvain*. fr. URL: https://www.uclouvain.be/fr/universite-transition/energie-patrimoine-bati (visited on 05/26/2026).

[38] *Le prix du gaz en Belgique (2026) : évolution en KWh | TotalEnergies Belgique*. fr. URL: https://totalenergies.be/fr/particuliers/le-prix-du-gaz-en-belgique (visited on 05/25/2026).

[39] *facteursdemissionCO.be*. URL: https://www.facteursdemissionco2.be/facteurs (visited on 05/26/2026).

[40] *Le campus du Sart Tilman chauffé grâce à la cogénération biomasse*. fr. URL: https://www.durable.uliege.be/cms/c_10382858/fr/le-campus-du-sart-tilman-chauffe-grace-a-la-cogeneration-biomasse (visited on 05/26/2026).

Appendix A

UCLouvain's internal data on the Stevin and Mercator buildings

All the data used in the calculations in this document can be found in the Google Drive folder accessible via the following link: `https://uclouvain-my.sharepoint.com/:f:/g/personal/ugo_maquet_student_uclouvain_be/IgCyuCE3mhSsRZWrj_pLHFpmARY927A7CPQIe8t1K5xpRys?e=Ggn0OD`

Appendix B

Annual Heating Consumption

Annual heating consumption - degree days and climate-normalised values - Stevin and Mercator (2017-2025)

Year	DD	Stevin real (MWh)	Stevin norm. (MWh)	Stevin spec. (kWh/m^2)	Mercator real (MWh)	Mercator norm. (MWh)	Mercator spec. (kWh/m^2)
2017	2064	713.8	756.3	91.7	362.2	383.8	63.6
2018	1896	732.1	844.5	102.4	318.2	367.0	60.8
2019	1963	675.3	752.4	91.2	319.7	356.2	59.0
2020	1674	560.1	731.7	88.7	299.1	390.8	64.8
2021	2113	719.4	744.6	90.3	394.5	408.3	67.7
2022	1742	578.6	726.4	88.1	309.8	388.9	64.5
2023	1830	485.8	580.6	70.4	272.9	326.1	54.0
2024	1942	511.5	576.0	69.8	236.6	266.4	44.2
2025	1973	520.0	576.4	69.9	261.6	290.0	48.1

Table B.1: Climate-normalised energy consumption of Stevin and Mercator

Annual K coefficient and equivalent U_{global} values - Stevin and Mercator (2017-2025)

Year	K Stevin	U_{global} Stevin (W/m^2K)	K Mercator	U_{global} Mercator (W/m^2K)
2017	0.0419	1.75	0.0291	1.21
2018	0.0468	1.95	0.0278	1.16
2019	0.0417	1.74	0.0270	1.12
2020	0.0406	1.69	0.0296	1.23
2021	0.0413	1.72	0.0309	1.29
2022	0.0403	1.68	0.0295	1.23
2023	0.0322	1.34	0.0247	1.03
2024	0.0319	1.33	0.0202	0.84
2025	0.0319	1.33	0.0220	0.92
Average before works	**0.0421**	**1.75**	**0.0290**	**1.21**
Average after works	**0.0320**	**1.33**	**0.0223**	**0.93**
Variation	−24.0%	−24.0%	−23.2%	−23.2%

Table B.2: Evolution of the K coefficient and equivalent U_{global} for Stevin and Mercator

Appendix C

Heating Consumption Raw Data

Monthly Heating Consumption Data – Stevin and Mercator (2017–2025)

All values are expressed in MWh. Data provided by UCLouvain technical services (ADPI/SEPI).

Stevin (SC04)

Month	**2017**	**2018**	**2019**	**2020**	**2021**	**2022**	**2023**	**2024**	**2025**
January	194.6	144.8	150.8	126.9	158.4	155.2	115.8	134.2	133.7
February	103.8	155.7	103.8	90.5	107.0	114.1	89.6	76.8	91.8
March	72.0	118.7	91.1	66.2	89.2	68.8	69.7	57.8	54.6
April	47.2	32.1	50.3	7.6	63.7	51.8	44.5	39.6	21.3
May	12.1	4.2	34.4	13.7	30.1	7.2	7.3	10.0	8.6
June	0.8	0.0	2.5	3.9	0.3	1.8	0.2	5.5	2.0
July	0.0	0.0	0.0	0.0	0.0	0.0	0.0	0.0	0.0
August	0.0	0.0	0.0	0.0	0.0	0.0	0.0	0.0	0.0
September	11.6	6.7	3.9	5.1	4.0	7.0	0.0	6.4	6.7
October	33.4	39.4	43.2	55.2	53.2	12.8	18.2	28.6	39.0
November	103.3	97.0	96.7	80.8	102.2	58.2	68.0	72.5	78.7
December	134.9	133.5	98.6	110.1	111.3	101.7	72.5	80.2	83.5
Total	**713.8**	**732.1**	**675.3**	**560.1**	**719.4**	**578.6**	**485.8**	**511.5**	**520.0**

Table C.1: Monthly heating consumption of Stevin (SC04), in MWh, 2017–2025

Mercator (SC10)

Month	**2017**	**2018**	**2019**	**2020**	**2021**	**2022**	**2023**	**2024**	**2025**
January	99.6	60.9	69.3	66.9	80.6	73.8	62.1	56.8	67.2
February	52.1	65.2	45.6	50.2	56.6	59.5	47.2	33.6	49.5
March	38.9	53.6	40.9	33.3	46.1	41.1	44.8	24.7	33.4
April	31.1	16.6	22.0	6.0	41.5	31.4	29.0	16.5	14.6
May	10.9	4.7	17.2	13.3	22.9	7.0	8.8	4.6	7.0
June	2.4	0.3	1.2	3.3	0.5	0.5	1.0	3.5	1.5
July	0.0	0.0	0.0	0.0	0.0	0.0	0.0	0.0	0.0
August	0.0	0.0	0.0	0.0	0.0	0.0	0.0	0.0	0.0
September	7.7	4.9	3.5	2.0	3.9	6.0	0.0	3.1	2.3
October	17.5	20.6	21.8	30.4	27.7	8.9	10.7	13.7	16.4
November	47.5	41.3	46.2	41.6	49.8	31.4	32.8	39.2	33.0
December	54.4	49.9	51.9	52.0	65.0	50.2	36.4	40.8	36.8
Total	**362.2**	**318.2**	**319.7**	**299.1**	**394.5**	**309.8**	**272.9**	**236.6**	**261.6**

Table C.2: Monthly heating consumption of Mercator (SC10), in MWh, 2017–2025

UNIVERSITÉ CATHOLIQUE DE LOUVAIN
Louvain School of Management

Place des Doyens, 1 bte L2.01.01, 1348 Louvain-la-Neuve
Boulevard Emile Devreux 6, 6000 Charleroi, Belgique
Chaussée de Binche 151, 7000 Mons, Belgique

www.uclouvain.be/lsm